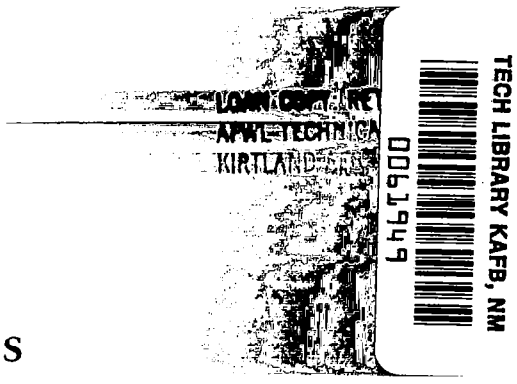

NASA Contractor Report 3334

Transient Dynamic Analysis of High-Speed Lightly Loaded Cylindrical Roller Bearings

I - Analysis

Thomas F. Conry

GRANT NSG-3098
JANUARY 1981

NASA

NASA Contractor Report 3334

Transient Dynamic Analysis of High-Speed Lightly Loaded Cylindrical Roller Bearings

I - Analysis

Thomas F. Conry
University of Illinois at Urbana-Champaign
Urbana, Illinois

Prepared for
Lewis Research Center
under Grant NSG-3098

NASA
National Aeronautics
and Space Administration

Scientific and Technical
Information Branch

1981

TABLE OF CONTENTS

	Page
SUMMARY	1
INTRODUCTION	2
THE CONSTITUENT MODELS	6
Load distribution in the rollers	12
Traction between the rollers and the races	19
Drag forces on the cage	23
Roller-cage interaction forces	26
Driving force between cage and land	33
Drag torque on the cylindrical roller surface	34
Drag torque on the roller ends	37
Forces between roller end and guiding flange	38
THE TWO DIMENSIONAL GOVERNING DIFFERENTIAL EQUATIONS OF MOTION	41
THE THREE DIMENSIONAL GOVERNING DIFFERENTIAL EQUATIONS OF MOTION	53
DISCUSSION OF RESULTS	64
CONCLUDING REMARKS	66
REFERENCES	67
LIST OF SYMBOLS	70

SUMMARY

The governing differential equations of motion for a high speed cylindrical roller bearing are developed under the assumptions that the bearing is isothermal and that the roller tilt and skew are very small. Two sets of differential equations are presented; the first which deals with planar motion of the roller bearing system, and the second which includes the effect of roller skewing. The equations as presented are in a format for programming on a digital computer.

INTRODUCTION

Current design trends for aircraft gas turbine engines are to achieve higher speeds and lighter weights. The primary advantages of these higher speeds and light weights are to increase payload and to reduce the drag induced by the externally mounted machines.

The mainshaft bearings used for high speed turbines are both cylindrical roller and ball bearings. The roller bearings have both high radial load capacity and the ability to permit relatively unconstrained axial motion under differential thermal expansion of the rotor when the engine is at operating condition. At high speeds and under low loads the rollers in the bearing have a tendency to slip or skew or both. These phenomena may cause the bearing to fail prematurely due to surface distress and/or jamming between the cage and the roller which can lead to catastrophic bearing failure.

In lightly loaded roller bearings operating at very high speeds, the rollers are subjected to centrifugal forces which keep them in contact with the outer race. The rollers are also subjected to contact forces as they traverse through the load zone of the bearing and react against the externally applied loads. These loading conditions, together with the effects of elastohydrodynamic lubrication, influence the rollers to slip relative to the races. As a consequence, the cage rotational speed falls below the theoretical epicyclic speed and, as the rollers traverse through the load zone, they are subjected to a varying radial force which

causes them to speed up and to slow down.

To understand the behavior of high speed lightly loaded roller bearings, it is necessary to examine the dynamic behavior of the rollers and the cage, and to determine the force interactions present in the bearing. Methods which are currently available are steady state force and moment balances. These analyses predict the average forces and moments on the rollers and cage. Transient effects such as cage whirl, roller slip as a function of angular position, or skewing cannot be predicted with any reasonable accuracy using these steady state methods. A time-domain solution to the differential equations of motion of the rollers and the cage in the bearing will provide detailed information on the cage-roller and roller-race interactions in the bearing. This detailed knowledge of the behavior of high speed roller bearings will aid engineers and engine designers in finding ways to improve their design with the objective of increasing roller bearing operating life and reliability.

Two articles have reported studies of the transient dynamic behavior of ball bearings. Walters [1] investigated the interaction between the cage and the ball while Gupta [2] investigated the ball-race dynamics without the effects of the bearing cage. Rumbarger, et al. [3] modeled the roller bearing and performed a steady state dynamic analysis on the resulting system of equations. The results of this study showed that the predicted cage slip compared favorably with experimental data on cage slip when the effective viscous drag forces of the lubricant on the cage were adjusted by varying the effective density of the lubricant.

Recently, Gupta [4] published a series of papers on the dynamic analysis of rolling element bearings. The approach to the problem utilized by Gupta is essentially the same as the approach utilized in this report. The work by both investigators was conducted independently and resulted in the same general approach to the problem. Most of the models in this report and in [4] are based on the work of Rumbarger et. al. [3].

The major assumption used in this work is that the bearing system is at a thermal steady state. This implies that the lubricant properties do not vary because of temperature changes and that the geometry of the rollers and races remains constant because of no thermal expansion. The motion of the rollers was assumed to be essentially planar. The tilt and skew angles of the roller are so small that they do not appreciably change the dynamics of motion of the roller, but the tilt and skew angles do have a dominant effect on the forces acting on the roller.

The purpose of this program of research was to achieve the following goals:

(1) To develop models which describe the interactions among forces, relative displacements and relative velocities between components in a cylindrical roller bearing and which are computationally efficient.

(2) To develop a working computer program for planar motion of the rollers and cage in the bearing which incorporates the models from goal (1).

(3) To develop the additional models and governing differential equations which describe the three dimensional motions of the rollers.

(4) To develop a working computer program for the three dimensional motion of the components of the bearing.

The above goals were met and the results are presented in the subsequent sections of this report. The governing relationships between forces and displacement and velocity for the many conditions present in roller bearings are presented in the section THE CONSTITUENT MODELS.

The governing differential equations of motion are developed for the two dimensional motion. Then the governing differential equations of motion for the three dimensional motion are derived. The assumptions upon which these equations are based together with the process of non dimensionalizing the equations are discussed.

The final section of this Part contains the conclusions and recommendations for further work. Part II [5] of this report contains the organization of the computer program and results obtained by using this program.

THE CONSTITUENT MODELS

The primary forces present in a high speed roller bearing are the normal forces between the roller and the races needed to balance the external forces and moments and the centrifugal forces on the rollers. Associated with these normal forces are the tractive forces between the rollers and the races.

The cage-roller interaction forces result from a lubricant squeeze film phenomenon and, in extreme cases, a contact phenomenon. The remaining forces are a result of shear stresses on the surfaces of the cage and rollers due to a shearing of the fluid medium.

The relationships between the forces and the deflections and relative velocities are based on the global coordinate system shown in Figure 1. The y axis is placed in a vertical position, parallel to the gravity vector, and z axis is parallel to the centerline of the shaft. The x axis is perpendicular to both the y and z axes. The angular velocities of the j'th roller and the cage are shown in Figure 2; $\dot{\zeta}_j$ is the angular velocity of the roller about its own axis, $\dot{\phi}_j$ is the angular velocity of the center of mass of the roller about the global z axis and $\dot{\vartheta}$ is the angular velocity of the cage about the global z axis. The forces and moments acting <u>on</u> a roller are shown in Figures 3 and 4. Figure 3 shows the net forces and torques projected on a plane normal to the z axis while Figure 4 shows the distribution of load between the roller and inner race and the roller and outer race together with the roller-guide flange impact forces (top view only). The net forces and torques acting on the cage are shown schematically in Figure 5. The net translational

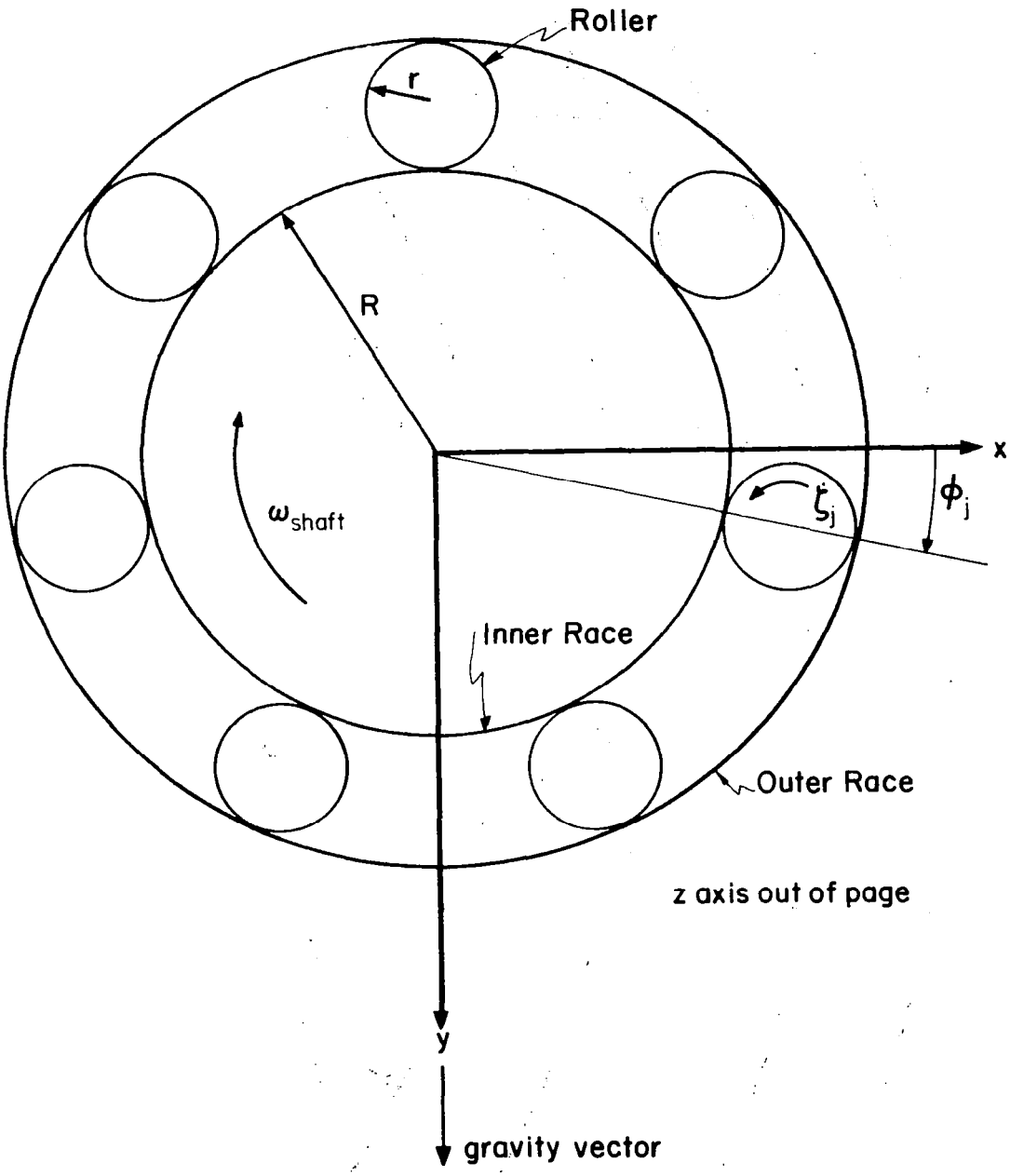

Figure 1. The Global Coordinate System for the Cylindrical Roller Bearing

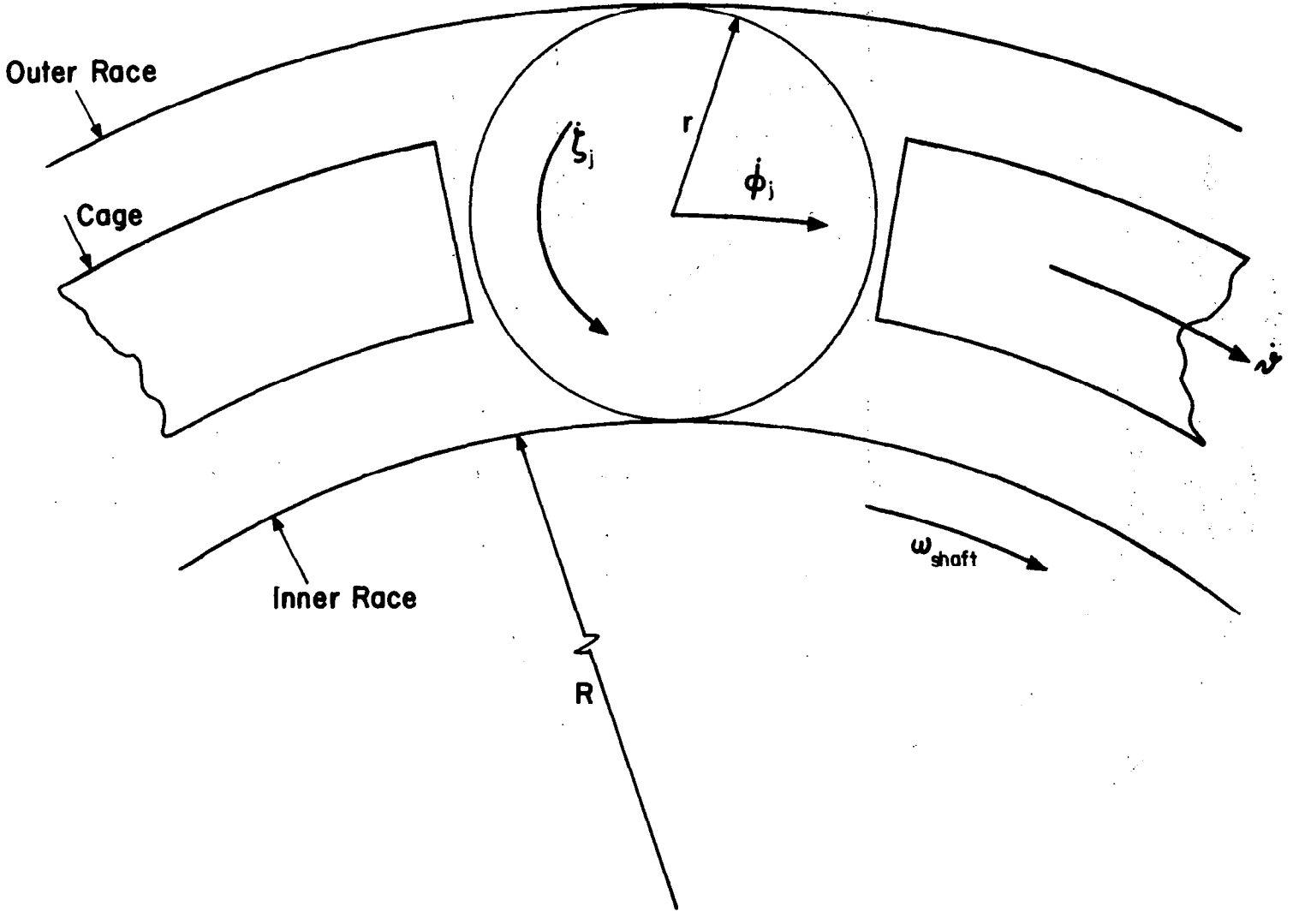

Figure 2. The Angular Velocities of the Roller and the Cage

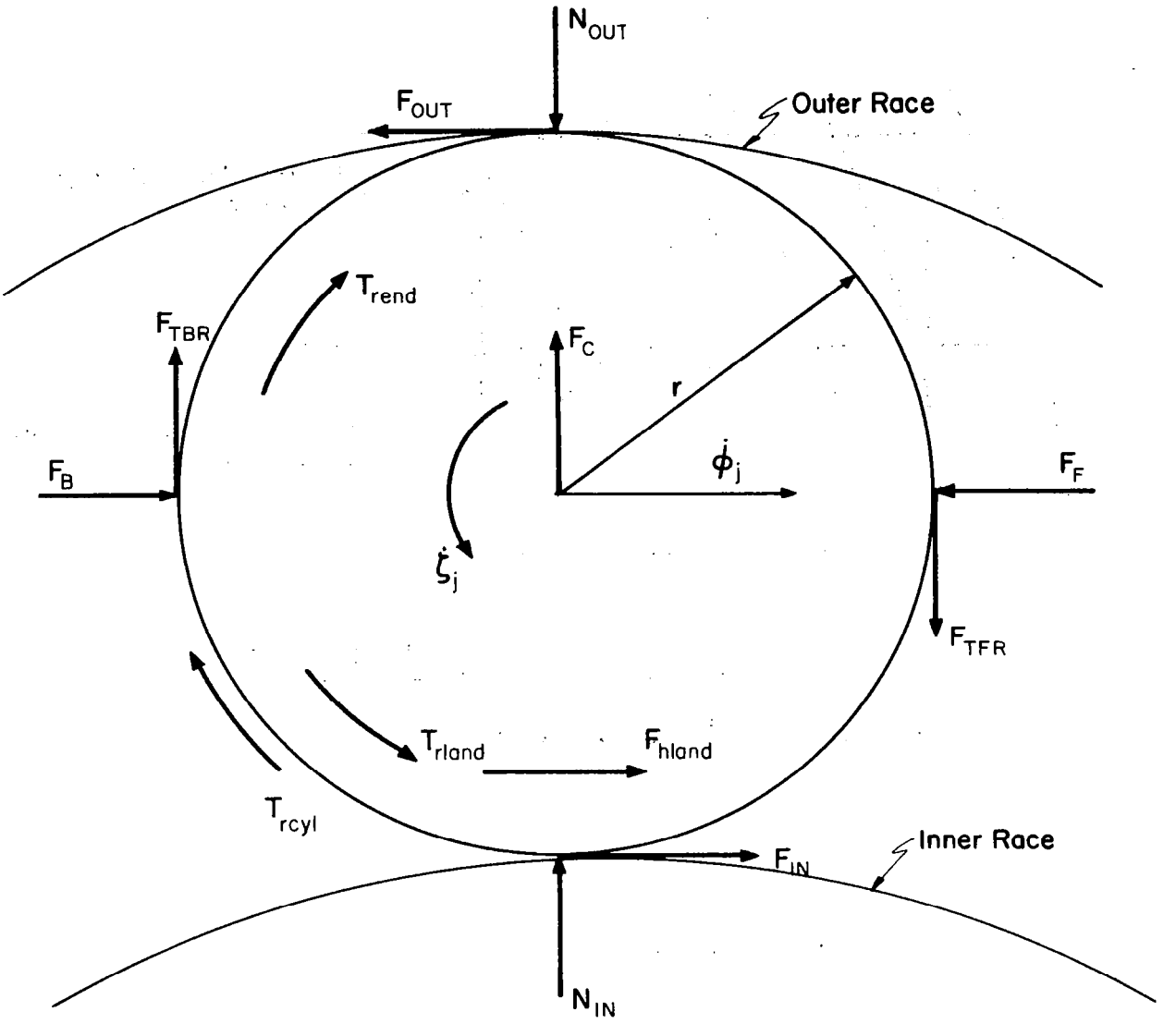

Figure 3. The Forces and Torques in Planes Normal to the z-Axis

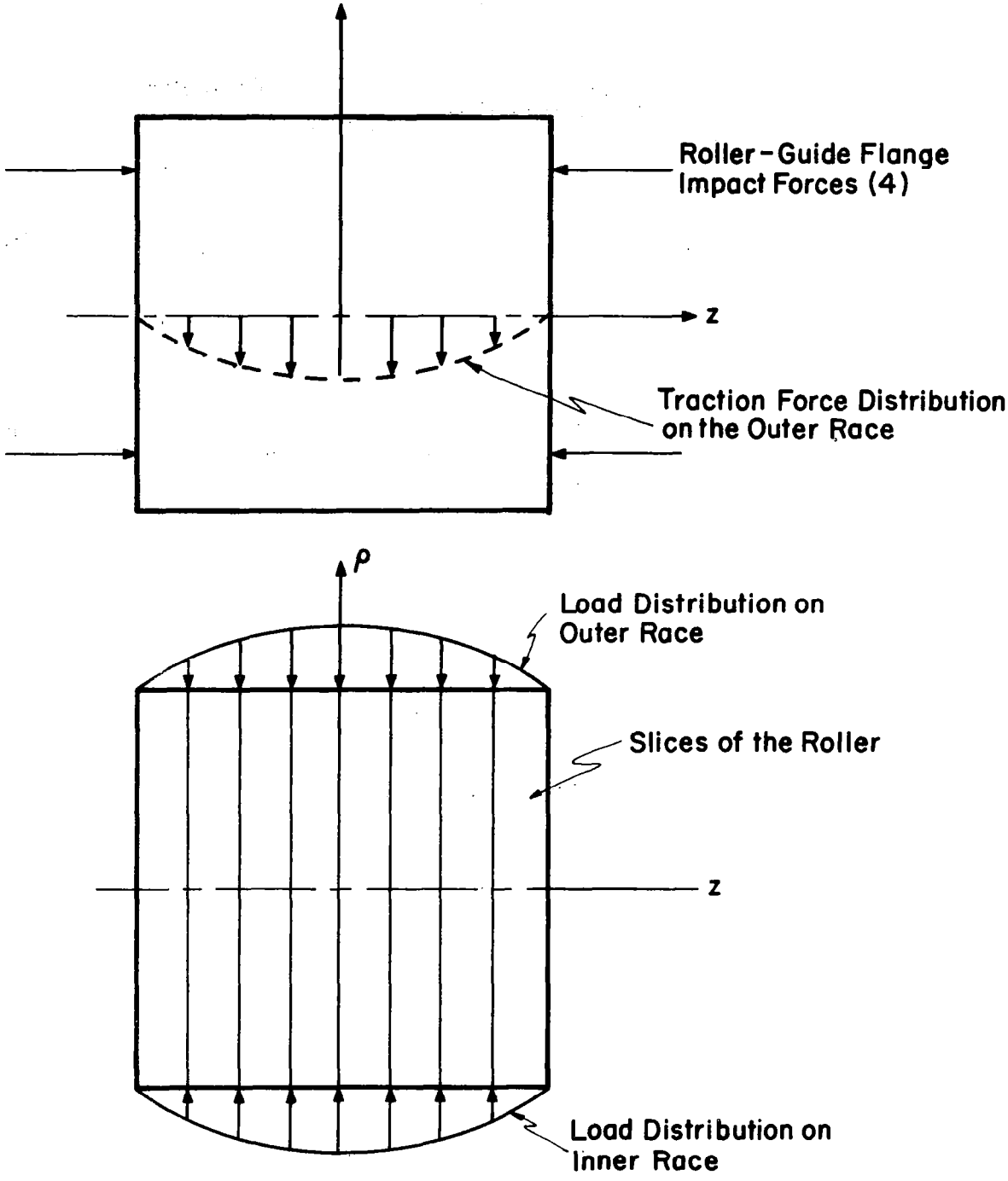

Figure 4. Roller-Race and Roller - Guide Flange Interaction Forces

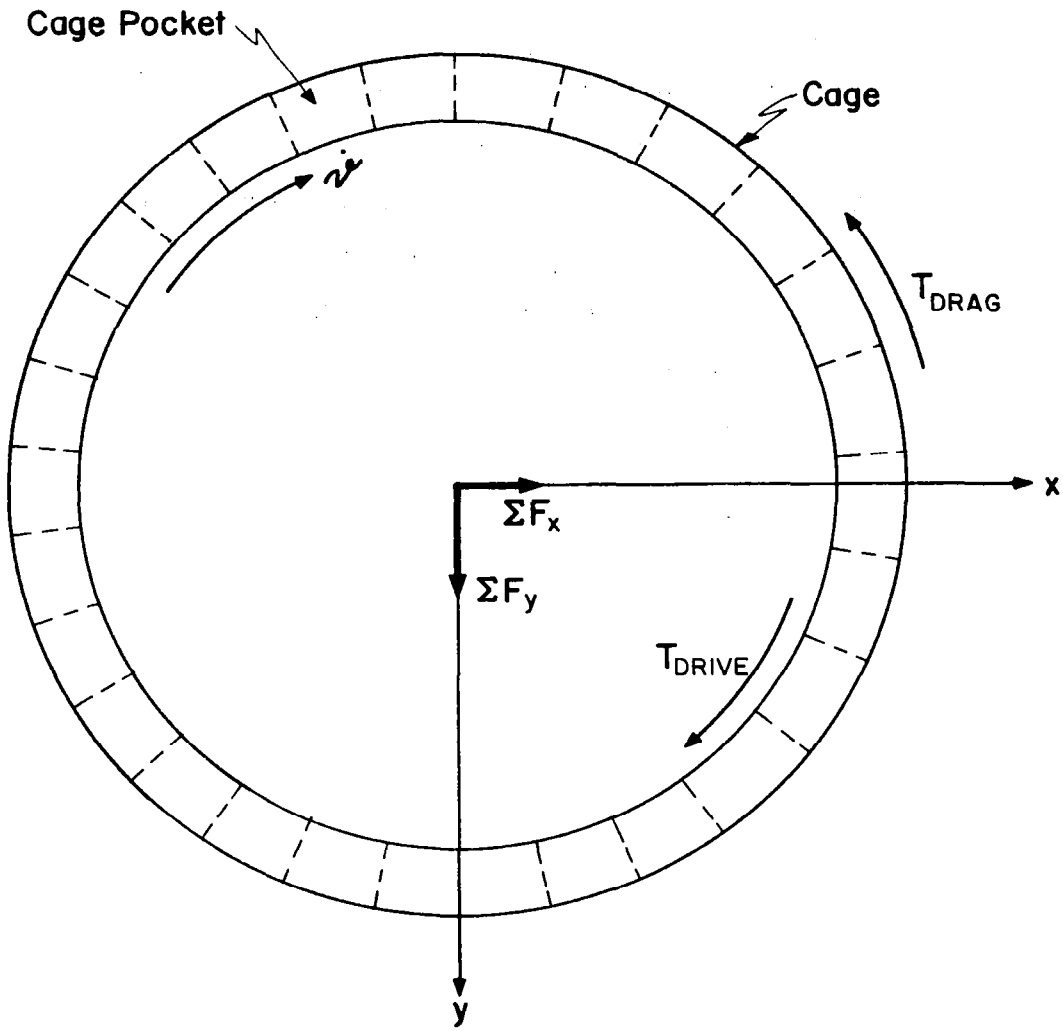

Figure 5. The Net Forces and Torques Acting on the Cage

forces, Σ_{Fx} and Σ_{Fy}, are the sum of the forces acting on the cage as a result of cage-roller interaction and cage-guide flange interaction. The torques T_{DRIVE} and T_{DRAG} are the sums of all the driving torques and drag torques respectively as a result of cage-roller interaction, cage-guide flange interaction and drag torques induced by the cage moving through the lubricant/air medium.

This section identifies each of these forces and presents the detailed relationships necessary to calculate them.

Load distribution in the rollers

When the spacing between the inner race and the outer race is less than the undeformed diameter of the roller, a normal contact pressure between the roller and the races is induced. The movement of the inner ring relative to the outer ring may be a result of directly applied external forces or overturning or misalignment moments. The contact pressure on the rollers will be symmetrical if the loading is due only to a directly applied radial force. If misalignment is present, the contact pressures will be non-symmetrical along the length of the roller. In this investigation only crowned rollers are considered.

This problem was investigated by Harris [6] and by Liu [7] who considered the effect of centrifugal force for high speed cylindrical roller bearings. The roller is divided into segments or "slices" along the axis and the contact pressures are determined over each of these segments, Figure 4. This provides an approximation to the non-uniform load distribution along the axis of a roller under misalignment.

The analysis is based on the work of Palmgren [8] which gives a relationship between the deformation (g) of a cylinder of length (ℓ) and an applied load (Q) as

$$g = A \frac{Q^{0.9}}{\ell^{0.8}} \tag{1}$$

where $A = 5.46 \times 10^{-8}$ for steel components. As the computer program will utilize displacements as the state variables, the above expression is inverted, utilizing a load intensity $\bar{q}$.

$$\bar{q} = \frac{Q}{\ell} \tag{2}$$

then

$$\bar{q} = \frac{g^{1.11}}{A^{1.11} \ell^{0.11}} \tag{3}$$

When the bearing is subjected to radial displacements Δ_x and Δ_y and angular misalignments θ_x and θ_y, the equations (13) and (14) in Liu [7] are replaced with the following expressions for the total contact deformations at the inner and outer contacts respectively at the center of the i^{th} slice of the j^{th} roller.

$$g_{1ij} = \Delta_x \cos\phi_j + \Delta_y \cos(\phi_j - \pi/2) + \left[z_i + R\,(1/2\,(\theta_y \cos\phi_j - \theta_x \sin\phi_j))\right] \cdot \left[\theta_y \cos\phi_j - \theta_x \sin\phi_j - \beta_j \operatorname{sign}(\cos(\phi_j + \pi/2 - \Phi_o))\right] - \frac{Pd}{2} - \delta^o_{\phi_j} - C_i \quad (4)$$

$$g_{2ij} = \delta^o_{\phi_j} + \left[z_i + R\,(1/2\,(\theta_y \cos\phi_j - \theta_x \sin\phi_j))\right] \left[\beta_j \operatorname{sign}(\cos(\phi_j + \pi/2 - \Phi_o))\right] - C_i \quad (5)$$

where C_i is the initial separation due to crowning

and P_d is the diametral clearance

and where Φ_o is given by the following relationship based on Ref. 5:

$$\Phi_o = \tan^{-1}\frac{\theta_y}{\theta_x} \quad (6)$$

if $\theta_x = 0$ and $\theta_y \geq 0$, $\Phi_o = \pi/2$

$\theta_x = 0$ and $\theta_y < 0$, $\Phi_o = -\pi/2$

Thus, using the conventions in Liu [7], the misalignment applied to any roller at any angular location ϕ_j is

$$\theta_j = \theta_y \cos\phi_j + \theta_x \cos(\phi_j + \pi/2) \quad (7)$$

The centrifugal force on a roller is given as (based on equation (17) in Liu [7])

$$F_c = \pi/8\ (\pi/30)^2\ \rho\ (2(R + r))\omega_c^2 \sum_{k=1}^{NP} (2r - 2C_k)^2 \qquad (8)$$

where ρ is the mass density of the roller

ω_c is the angular velocity of the cage

C_k is the roller crown drop at segment k as defined for equation (4)

The load distribution on the rollers in the bearing is determined by enforcing the conditions of static equilibrium of forces and moments on each of the rollers. The diametral clearance, initial separations due to crowning and linear and angular deformations of the inner race with respect to the outer race (Δ_x, Δ_y, θ_x, θ_y) are given as inputs to the calculation. The computational procedure will give the central deformation of the roller, $\delta^o_{\phi_j}$, and the angular displacement of the roller, β_j, for all the rollers. The contact pressure distributions are then calculated using the $\delta^o_{\phi_j}$'s and the β_j's. The net load and moment on the bearing can be determined from equilibrium considerations of the inner contact forces on the inner race.

The static equilibrium of force on the roller implies that the sum of the forces at the inner contact and the centrifugal force must balance the forces at the outer contact. Setting these sums equal to a residual (F_j) gives

$$F_j = \sum_{i=1}^{NP} \left[\frac{w}{A^{1.11}\, \ell^{0.11}} (g_{1ij})^{1.11} - \frac{w}{A^{1.11}\, \ell^{0.11}} (g_{2ij})^{1.11} \right] + F_c \qquad (9)$$

$$j = 1, \ldots, NZ$$

The static equilibrium of moments on the roller implies that the sum of the moments of the inner contact forces must balance the sum of the moments of the outer contact forces. Setting these sums equal to a residual F_{j+NZ} gives

$$F_{j+NZ} = \sum_{i=1}^{NP} \left[\frac{w\, z_i}{A^{1.11}\, \ell^{0.11}} (g_{1ij})^{1.11} - \frac{w\, z_i}{A^{1.11}\, \ell^{0.11}} (g_{2ij})^{1.11} \right] \qquad (10)$$

$$j = 1, \ldots, NZ$$

where NZ is the number of rollers

NP is the number of slices along the axis of the roller

w is the width of a slice = $\frac{\ell}{NP}$

When the state of static equilibrium is reached, the residuals will be reduced to zero. This is a system of (2 X NZ) nonlinear algebraic equations in the NZ variables $\delta\phi_j^{\circ}$ and the NZ variables β_j.

Defining

$$\Gamma = \frac{w}{A^{1.11}\, \ell^{0.11}} \qquad (11)$$

equations (9) and (10) become

$$F_j = \Gamma \sum_{i=1}^{NP} \left[(g_{1ij})^{1.11} - (g_{2ij})^{1.11} \right] + F_c \qquad (12)$$

$$j = 1, \ldots, NZ$$

$$F_{j+NZ} = \Gamma \sum_{i=1}^{NP} \left[z_i \, (g_{1ij})^{1.11} - z_i \, (g_{2ij})^{1.11} \right] \qquad (13)$$

$$j = 1, \ldots, NZ$$

A Newton-Raphson procedure is used to solve this system of equations. The derivatives of the residual functions to be used in the Jacobian matrix are given as:

$$\frac{\partial F_j}{\partial \beta_k} = 0 \qquad \text{if } k \neq j$$

$$= 1.11 \Gamma \sum_{i=1}^{NP} \left\{ -(g_{1ij})^{0.11} - (g_{2ij})^{0.11} \right\} \cdot \left\{ \left[z_i + \frac{R}{2} \, (\theta_y \cos \phi_j - \theta_x \sin \phi_j) \right] \cdot \text{sign} \left(\cos \left(\phi_j + \pi/2 - \Phi_o \right) \right) \right\} \qquad (14)$$

$$\text{if } k = j$$

$$\frac{\partial F_j}{\partial \delta \phi_k^o} = 0 \qquad \text{if } k \neq j$$

$$= 1.11 \sum_{i=1}^{NP} \left[-(g_{1ij})^{0.11} - (g_{2ij})^{0.11} \right] \cdot \Gamma \qquad (15)$$

$$\text{if } k = j$$

$$\frac{\partial F_{j+NZ}}{\partial \beta_k} = 0 \qquad \text{if } k \neq j$$

$$= 1.11 \left[\sum_{i=1}^{NP} \left\{ -z_i \left(g_{1ij}\right)^{0.11} - z_i \left(g_{zij}\right)^{0.11} \right\} \right. \tag{16}$$

$$\cdot \left\{ \left[z_i + \frac{R}{2} \left(\theta_y \cos \phi_j - \theta_x \sin \phi_j \right) \right] \right.$$

$$\left. \left. \cdot \text{ sign } \left(\cos \left(\phi_j + \frac{\pi}{2} - \Phi_o \right) \right) \right\} \right] \qquad \text{if } k = j$$

$$\frac{\partial F_{j+NZ}}{\partial \delta\phi_k^o} = 0 \text{ if } k \neq j \tag{17}$$

$$= 1.11 \left[\sum_{i=1}^{NP} \left[-z_i \left(g_{1ij}\right)^{0.11} - z_i \left(g_{zij}\right)^{0.11} \right] \right] \text{ if } k = j$$

Denoting changes in the values of β_j and $\delta\phi_j^o$ by $\delta\beta_j$ and $\delta\delta\phi_j^o$ respectively, the system of equations to be solved is of the form:

$$\begin{bmatrix} \left[\frac{\partial F_j}{\partial \beta_k}\right] & \left[\frac{\partial F_j}{\partial \delta\phi_k^o}\right] \\ \left[\frac{\partial F_{j+NZ}}{\partial \beta_k}\right] & \left[\frac{\partial F_{j+NZ}}{\partial \delta\phi_k^o}\right] \end{bmatrix} \begin{bmatrix} \left[\delta\beta_j\right] \\ \left[\delta\delta\phi_j^o\right] \end{bmatrix} = \begin{bmatrix} -\left[F_j\right] \\ -\left[F_{j+NZ}\right] \end{bmatrix} \tag{18}$$

The submatrices in the coefficient matrix are diagonal, so the solution of the above system of 2 X NZ equations in 2 X NZ unknowns can be reduced to the solution of NZ (2 X 2) systems of equations. A solution may be obtained very efficiently. This procedure is programmed in subroutine ROLDIS [5] and its subsidiary subroutines.

The total normal forces on the roller at the inner race and the outer race are then given as:

$$N_{in}^{(j)} = \sum_{i=1}^{NP} \frac{w}{A^{1.11}\,\ell^{0.11}} \left(g_{1ij}\right)^{1.11}$$

$$N_{out}^{(j)} = \sum_{i=1}^{NP} \frac{w}{A^{1.11}\,\ell^{0.11}} \left(g_{2ij}\right)^{1.11} \qquad (19)$$

$$j = 1, \ldots, NZ$$

Traction between the rollers and the races

The tractive forces in an EHD contact between a roller and a race are dependent on the lubricant formulation, the Hertzian contact pressure, the rolling velocity, the sliding velocity and the temperature of the surfaces. Experimental evidence, e.g. [9], has shown that the tractive forces are not directly proportional to the shear rate of the lubricant over a wide range of shearing rates. For a constant maximum Hertzian pressure and rolling velocity, the traction force rises, peaks and then decreases with increasing sliding velocity.

An approximate model which was utilized for the development of the roller bearing dynamics computer program is based on a curve of normalized traction coefficient versus normalized sliding speed. This curve was presented in Ref. [10] for a Mil L-7808 oil.

The model is a piecewise linear approximation to the above referenced curve which is presented in Fig. 6. The normalizing constants μ^* and u_s^* are given as [10]:

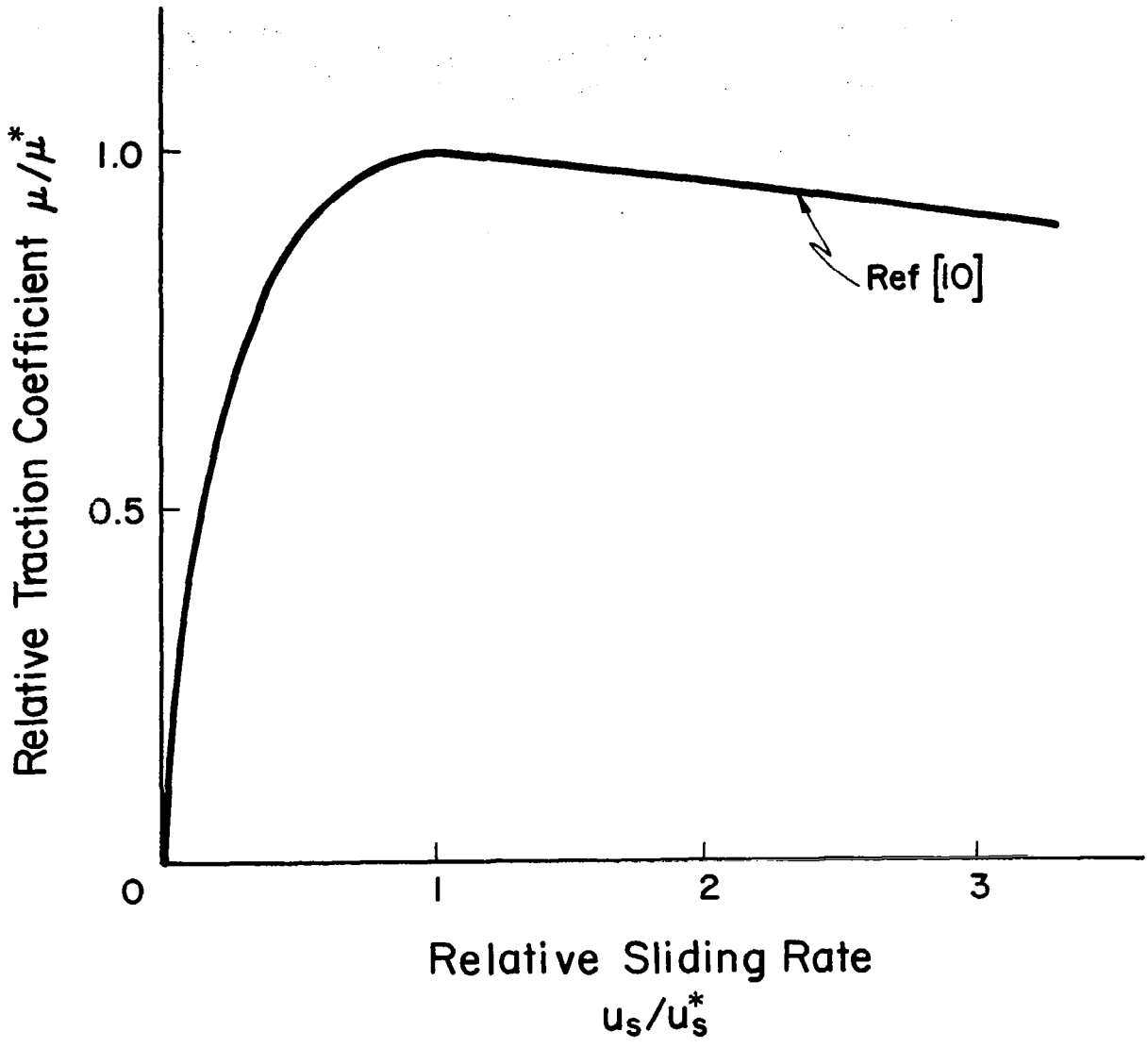

Figure 6. Normalized Traction Curve for Mil-L-7808 Oil

$$\frac{\mu^*}{\mu_b^*} = \left(\frac{f(q_o)}{1.33 \times 10^4} \right)^{0.61} \left(\frac{8.2736 \times 10^8}{q_o} \right)^{1.14} \left(\frac{\nu_o}{15 \times 10^{-6}} \right)^{0.28} \left(\frac{11.43}{v} \right)^{0.46} \quad (20)$$

$$\frac{u_s^*}{u_{s_b}^*} = \left(\frac{1.33 \times 10^4}{f(q_o)} \right)^{0.39} \left(\frac{8.2736 \times 10^8}{q_o} \right)^{0.28} \left(\frac{15 \times 10^{-6}}{\nu_o} \right)^{0.70} \left(\frac{v}{11.43} \right)^{0.56} \quad (21)$$

$$f(q_o) = 0.802 \quad (q_o \times 10^{-8})^{4.598123} \quad (22)$$

where q_o is the maximum Hertz contact pressure (n/m^2)

u_s is the sliding velocity at a roller/race contact (m/s)

u_s^* is the normalizing value of u_s

$u_{s_b}^*$ is the base value of the relative sliding velocity upon which the correlation is based. (For Mil L-7808 oil, $u_{s_b}^* = 1.397$ m/s

v is the rolling velocity at the roller/race contact (m/s)

ν_o is the oil viscosity at operating temperature (m^2/s)

μ is the traction coefficient

μ^* is the maximum value of the traction coefficient corresponding to u_s

μ_b^* is a base value of the traction coefficient upon which the correlation is based. (For Mil L-7808 oil, $\mu_b^* = 0.019$).

The traction coefficient is given by the following model:

$$0 \leq \frac{u_s}{u_s^*} \leq 0.25$$

$$\frac{\mu}{\mu^*} = 2.80 \frac{u_s}{u_s^*}$$

$$0.25 \leq \frac{u_s}{u_s^*} \leq 0.50$$

$$\frac{\mu}{\mu^*} = 0.70 + 0.80 \left(\frac{u_s}{u_s^*} - 0.25 \right)$$

$$0.50 \leq \frac{u_s}{u_s^*} \leq 0.75$$

$$\frac{\mu}{\mu^*} = 0.90 + 0.30 \left(\frac{u_s}{u_s^*} - 0.50 \right) \qquad (23)$$

$$0.75 \leq \frac{u_s}{u_s^*} \leq 1.00$$

$$\frac{\mu}{\mu^*} = 0.975 + 0.10 \left(\frac{u_s}{u_s^*} - 0.75 \right)$$

$$1.00 \leq \frac{u_s}{u_s^*}$$

$$\frac{\mu}{\mu^*} = 1.00 - 0.0571 \left(\frac{u_s}{u_s^*} - 1.00 \right)$$

$$\frac{u_s}{u_s^*} > 15$$

$$\frac{\mu}{\mu^*} = 1.00 - 0.0571 \left(15.0 - 1.0 \right)$$

Although this model is an approximation, it fairly represents the traction phenomenon in an EHD contact with Mil L-7808 oil. Other models can be utilized in the roller bearing dynamics program for different oils merely by changing a subroutine. The above equations are programmed in the function subroutine COEFF [5].

The traction force between the rollers and the race is of the form

$$F_{IN} = \mu_{in} N_{in}$$
$$F_{OUT} = \mu_{out} N_{out} \qquad (24)$$

Drag forces on the cage

As the cage rotates in the bearing it is subjected to forces which accelerate its motion and to forces which retard its motion. This section is devoted to the description of those forces which retard the motion of the cage excluding those caused by cage/roller interaction.

These drag forces are induced by the shearing of the air/oil mist mixture enveloping the cage of a high speed bearing. They are considered to act on the outer and the side surfaces of the cage.

Boness [11] experimentally described and analytically discussed the influence of the amount of lubricant supply on cage and roller motion in high speed roller bearings. Poplawski [12] introduced a fluid churning loss and cage pilot surface friction formulations. Rumbarger et. al. [3] extended Poplawski's approach and further examined the influence of fluid drag forces on individual surfaces of the cage.

The models used in this computer program are taken from Rumbarger et. al. [3]. The drag torques acting on the outer cylindrical surface of the cage are described by an equation of the form

$$T_{CDO} = \tau_w A r_{OUT} \tag{25}$$

where T_{CDO} is the drag torque on the surface

τ_w is the wall shear stress

A is the surface area

r_{OUT} is the outer radius of the cage

The wall stress for a surface rotating in a viscous fluid is defined by [13].

$$\tau_w = \frac{f \rho u^2}{2} \tag{26}$$

where f is a friction factor

ρ is the fluid density

u is the mass average velocity of the fluid

and $u = \frac{r_{OUT}}{2} \dot{\vartheta}$ for this correlation.

where $\dot{\vartheta}$ is the angular velocity of the cage.

The effective density of the oil/air mixture about the cage is given in [3] as

$$\rho_{eff} = \frac{\rho \ (DECFUL)^2}{(0.4 + 0.6 \ DECFUL)} \tag{27}$$

where DECFUL is the ratio of the oil volume in the bearing to the total volume of the bearing.

ρ is the density of the oil

ρ_{eff} is the effective density

The Couette turbulence regime is assumed for the outer surface, thus

$$\frac{f}{f_L} = 3.0 \left[\frac{N_{RE}}{2500}\right]^{0.85596} \tag{28}$$

where

$$N_{RE} = \frac{r_c \omega c}{\nu} \tag{29}$$

and

$$f_L = \frac{16}{N_{RE}} \tag{30}$$

Here N_{RE} is the Reynolds number

f_L is the laminar friction factor

If the Reynolds number is less than 2500 or the Taylor number is less than 41, the appropriate friction factor is taken to be the laminar friction factor f_L. The Taylor number is defined as

$$N_{TA} = \frac{r_c \omega c}{\nu} \sqrt{\frac{c}{r_c}} \tag{31}$$

where r_c is a characteristic radius, equal to r_{OUT}

ω is the angular velocity, equal to $\dot{\vartheta}$

c is a radial clearance

ν is the oil kinematic viscosity

For the side walls of cages, the characteristic radius to be used in the correlations below is modified by using the relationship

$$r_c^5 = r_{OUT}^3 \left(r_{OUT}^2 - r_{IN}^2\right) \tag{32}$$

where r_{OUT} is the outer radius

r_{IN} is the inner radius

The Reynolds number is given in this case as:

$$N_{RE} = \frac{r_c^2 \omega}{\nu} \tag{33}$$

and the drag torque on the sides is given as

$$T_{CDS} = \frac{1}{2} \rho \omega^2 r_c^5 C_N \tag{34}$$

where

$$C_N = \begin{cases} \dfrac{3.87}{(N_{RE})^{1/2}} & \text{for laminar flow, } N_{RE} < 300{,}000 \\ \dfrac{0.146}{(N_{RE})^{1/5}} & \text{for turbulent flow } N_{RE} > 300{,}000 \end{cases} \tag{35}$$

These relationships are programmed in subroutine CGTRQ [5].

Roller-cage interaction forces

In roller bearings the rollers have the freedom to move relative to the cage. In the load zone, the roller may be accelerated and approach the front part of the pocket resulting in a driving force on the cage. Outside of the load zone the roller may start to slip, decelerate and then approach the rear part of the pocket resulting in a retarding force on the cage. In many instances the squeeze film forces in the lubricant which are generated by the relative approach of the roller and the cage are not large because of the relative freedom of motion of all the components of the bearing.

If the force was too large, the cage would accelerate or decelerate until an equilibrium could be reached between all the rollers and the cage.

The model which was used in the computer program is that given by Dowson, Markho and Jones [14]. This model describes the lubrication of lightly loaded rigid cylinders by an isoviscous lubricant in combined rolling, sliding and normal motion, Fig. 7 . The governing equation is the Reynolds equation with side-leakage neglected. The boundary conditions used for this model are:

at the inlet, the pressure is zero;

at the outlet, the pressure and the pressure gradient are zero.

The normal pressure distribution is computed and from this the normal force and traction forces are determined. Dowson, Markho and Jones presented their results and gave regression equations for the instantaneous load carrying capacity and the surface tractions. The data given are ideal for inclusion in the roller bearing dynamics program because of the relative ease in calculating the regression equations.

The expression for the instantaneous load carrying capacity is

$$N = \frac{4.896}{H_o}\left[\, 1.0 - 1.89351\, q + 1.54192\, q^2 - 0.33529\, q^3 - 0.17678\, q^4 - 2.85050\, q\, H_o + 1.73361\, q^2\, H_o \right] \quad (36)$$

$$\text{if } q \geq 0$$

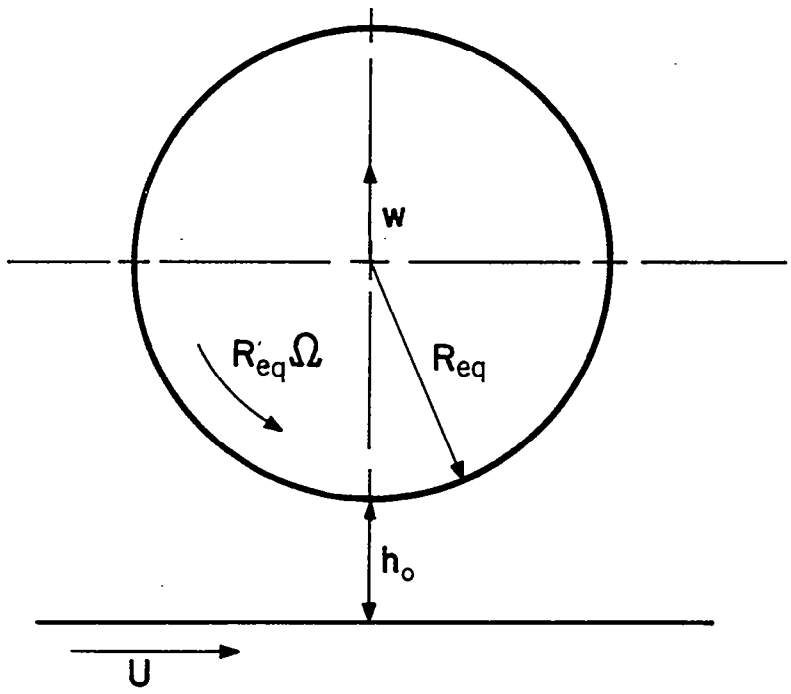

Figure 7. Model of a Rigid Cylinder Impacting a Surface with Combined Rolling, Sliding and Normal Motion

$$N = \frac{4.896}{H_o} \left[1.0 - 1.87439\ q + 1.70716\ q^2 + 0.62039\ q^3 + 0.04271\ q^4 - 3.31298\ q\ H_o + 1.35849\ q^2\ H_o\right] \quad (37)$$

$$\text{if } q < 0$$

where N is the dimensionless normal load carrying capacity per unit length of cylinder $= \frac{n}{\mu u}$

q is the dimensionless (normal/entraining) velocity parameter $= \frac{w}{u} \left(\frac{R_{eq}}{2\ h_o}\right)^{1/2}$

H_o is the dimensionless minimum film thickness $= \frac{h_o}{R_{eq}}$

n is the normal load per unit length of the cylinder

μ is the dynamic viscosity of the lubricant

u is the entraining velocity $= \frac{U + R_{eq}\Omega}{2}$

w is normal velocity of the cylinder

R_{eq} is the radius of the geometrically equivalent cylinder near the plane.

Ω is the angular velocity of the cylinder

The surface traction acting on the roller is given by

$$F_{roller} = \frac{1}{H_o^{1/2}} \left[B - C\ \bar{v}\right] \quad (38)$$

The surface traction acting on the cage pocket surface is given by

$$F_{cage} = \frac{1}{H_o^{1/2}} \left[B + C\ \bar{v}\right] \quad (39)$$

where F_{roller} and F_{cage} are dimensionless tangential surface forces arising from viscous stresses = $\frac{f}{\mu u}$

B, C are constants which are defined below

$\bar{v}$ is the dimensionless sliding ratio = $2\left(\frac{U - R_{eq}\Omega}{U + R_{eq}\Omega}\right)$

The constants B and C are defined as follows:

$$B = (B)_{q=0}\left[1 - 0.76128\ q - 0.00358\ q^2 + 0.42000\ q^3 - 0.21924\ q^4 - 60.53144\ q\ H_o + 19.56741\ q^2\ H_o\right] \quad (40)$$

$$\text{if } q \geq 0$$

$$B = (B)_{q=0}\left[1 - 0.76443\ q - 0.02328 + 0.37387\ q^3 + 0.17758\ q^4 - 60.92918\ q\ H_o - 21.20263\ q^2\ H_o\right] \quad (41)$$

$$\text{if } q < 0$$

where

$$(B)_{q=0} = 4.5685 - 681.56\ H_o + 341795\ H_o^2 \quad (42)$$

$$C = (C)_{q=0}\left[1 - 0.19300\ q + 0.08479\ q^2 + 0.33245\ q^3 - 0.11347\ q^4 - 4.03120\ q\ H_o + 5.55690\ q^2\ H_o\right] \quad (43)$$

$$\text{if } q \geq 0$$

$$C = (C)_{q=0} \left[1 - 0.19648\ q + 0.07182\ q^2 + 0.19631\ q^3 + 0.08557\ q^4 - 3.71562\ q\ H_o - 1.15432\ q^2\ H_o\right] \quad (44)$$

$$\text{if } q < 0$$

where

$$(C)_{q=0} = 3.4843 - 113.66\ H_o + 56903\ H_o^2 \quad (45)$$

These expressions are generally valid for the range of values of the variables (q) and (H_o) of

$$-1.0 \leq q \leq +0.75$$

$$10^{-6} \leq H_o \leq 10^{-3}$$

When the variable H_o goes below 10^{-6}, the model is switched over to a Hertz contact model given by Loo [15] and linearly approximated by Conry and Seireg [16] for two cylinders in contact:

$$P' = \left(\frac{\pi E}{2(1-\nu^2)}\right)\left(\frac{1}{12.5}\right) w_H \quad (46)$$

where P' is the normal force per unit width of the roller resulting from the indentation w_H

w_H is the indentation of the cage by the cylinder

E is the modulus of elasticity of the roller and the cage

ν is Poisson's ratio

The indentation of the cage by the cylinder is measured from the point where $H_o = 1.0 \times 10^{-6}$ and the resulting normal force per unit width (P') is added to the normal force per unit width (n) evaluated at $H_o = 1.0 \times 10^{-6}$ in equations (36) and (37).

The minimum film thickness and the indentation (if any) of the roller relative to the cage in the cage pocket is defined as

$$h_o = \frac{C_g}{2} - d \qquad (47)$$

$$\text{if } \frac{h_o}{R_{eq}} \geq 10^{-6}$$

and

$$w_H = \left| h_o - 1.0 \times 10^{-6} R_{eq} \right| \qquad (48)$$

$$\text{if } \frac{h_o}{R_{eq}} < 10^{-6}$$

where C_g is the circumferential clearance in the cage pocket

R_{eq} is the equivalent radius of the roller and cage pocket surface

d is the displacement of the center of the roller from the center of the cage pocket.

The surface tractions acting on the surfaces of the cage pocket and the roller are taken to be the total normal force times a Coulomb friction constant of 0.05 when $H_o < 10^{-6}$.

These relationships are programmed in subroutine DIFFUN [5] with equations (36) to (45) programmed in subroutines RLCGF and FRICTF [5].

Driving force between cage and land

The roller bearing type considered in this report has a cage which rides on two inner race lands. Under full hydrodynamic lubrication, the relative motion between the cage and the inner race land gives rise to a pressure distribution between the inner surfaces of the cage and the land surfaces upon which it rides. The expression for the pressure distribution in this oil film is given by Kirk and Gunter [17].

The cage riding on an oil film between it and the inner race land can be modeled as an inside out journal bearing. The "journal" motion is prescribed while the "bearing" (in this case, the cage) moves in a path subject to the Newtonian equations of motion for the cage.

The expression for the forces acting on the cage is based on equation 3.42 of [17], but modified to consider prescribed displacements and velocities of the inner race.

$$\begin{Bmatrix} F_x \\ F_y \end{Bmatrix} = -\mu\, r_{OUT}\, L^3 \int_0^{2\pi} \frac{\left[(\omega_{shaft}+\omega_c)\left(-(x-\Delta_x)\sin\theta + (y-\Delta_y)\cos\theta\right) - 2.0\left(-(\dot{x}-\dot{\Delta}_x)\cos\theta - (\dot{y}-\dot{\Delta}_y)\sin\theta\right)\right]}{\left[C + (x-\Delta_x)\cos\theta + (y-\Delta_y)\sin\theta\right]^3} \cdot \begin{Bmatrix} \cos\theta \\ \sin\theta \end{Bmatrix} d\theta \qquad (49)$$

where F_x and F_y are the hydrodynamic forces on the cage

μ is the dynamic viscosity of the lubricant

L is the half-width of the total cage/land surface

ω_{shaft} is the angular speed of the inner race

ω_c is the angular speed of the cage

x and y are the displacements of the cage relative to a fixed frame

Δ_x and Δ_y are the displacements of the inner race relative to a fixed frame

C is the radial clearance between the cage and the inner race land

The integral in equation (49) is evaluated by a composite Legendre - Gauss quadrature using a 96 - point formula. This evaluation is performed subject to the restriction that the argument of the integral is negative. If it is positive, it is set to zero over that interval for purposes of the numerical integration. This corresponds to integrating over the positive pressure region only.

These expressions are programmed in subroutines DIFFUN, CGPRES and GQU3Z [5].

Drag torque on the cylindrical roller surface

As the roller spins about its own axis a shear stress is generated on the surface as a result of the shearing of the lubricant/air mixture present in the open spaces of the bearing. When summed over the cylindrical area and multiplied by the value of the radius of the roller, the drag torque is obtained. This model for the drag torque on the roller is given in Rumbarger et. al. [3] and is based on a vortex-turbulent correlation.

Before any quantities can be computed, the average clearance between the roller and the cage and between the roller and the race lands must be determined, Fig. 8. For this computer program the clearance between the roller and the cage was left out of this averaging process as the drag between the roller and cage was considered in a previous section. This clearance is defined by equation (50) and is the average clearance over the regions I, II, IV and V shown in Fig. 8.

$$C_H = \frac{1}{(2\pi - 4\theta_2)} \int_{\substack{\text{circumference} \\ \text{not adjacent} \\ \text{to the cage}}} C(\theta)\,d\theta \qquad (50)$$

The average clearance is then computed as:

$$C_H = 2\left[r\left(\ln\sqrt{\frac{1+\sin\theta_1}{1-\sin\theta_1}} - \theta_1\right) + \left(\frac{r+\frac{1}{2}C_g}{2}\right)\left(\ln\frac{1+\cos\theta_1}{1-\cos\theta_1} - \ln\frac{1+\sin\theta_2}{1-\sin\theta_2}\right) - r\left(\frac{\pi}{2} - \theta_1 - \theta_2\right)\right] \Big/ (\pi - 2\theta_2) \qquad (51)$$

where θ_1 and θ_2 are defined in Figure 8

and where C_g is the total circumferential clearance between the roller and the cage pocket as shown in Fig. 8.

The vortex-turbulent correlation was utilized by inserting the appropriate values of clearance, viscosity, speed and roller geometry into equations (29), (30) and (31) which give the Reynolds number, the laminar friction factor and the Taylor number respectively. The vortex turbulent correlation is given as [3].

$$\frac{f}{f_L} = 1.3\left[\frac{N_{TA}}{41}\right]^{0.539474} \qquad (52)$$

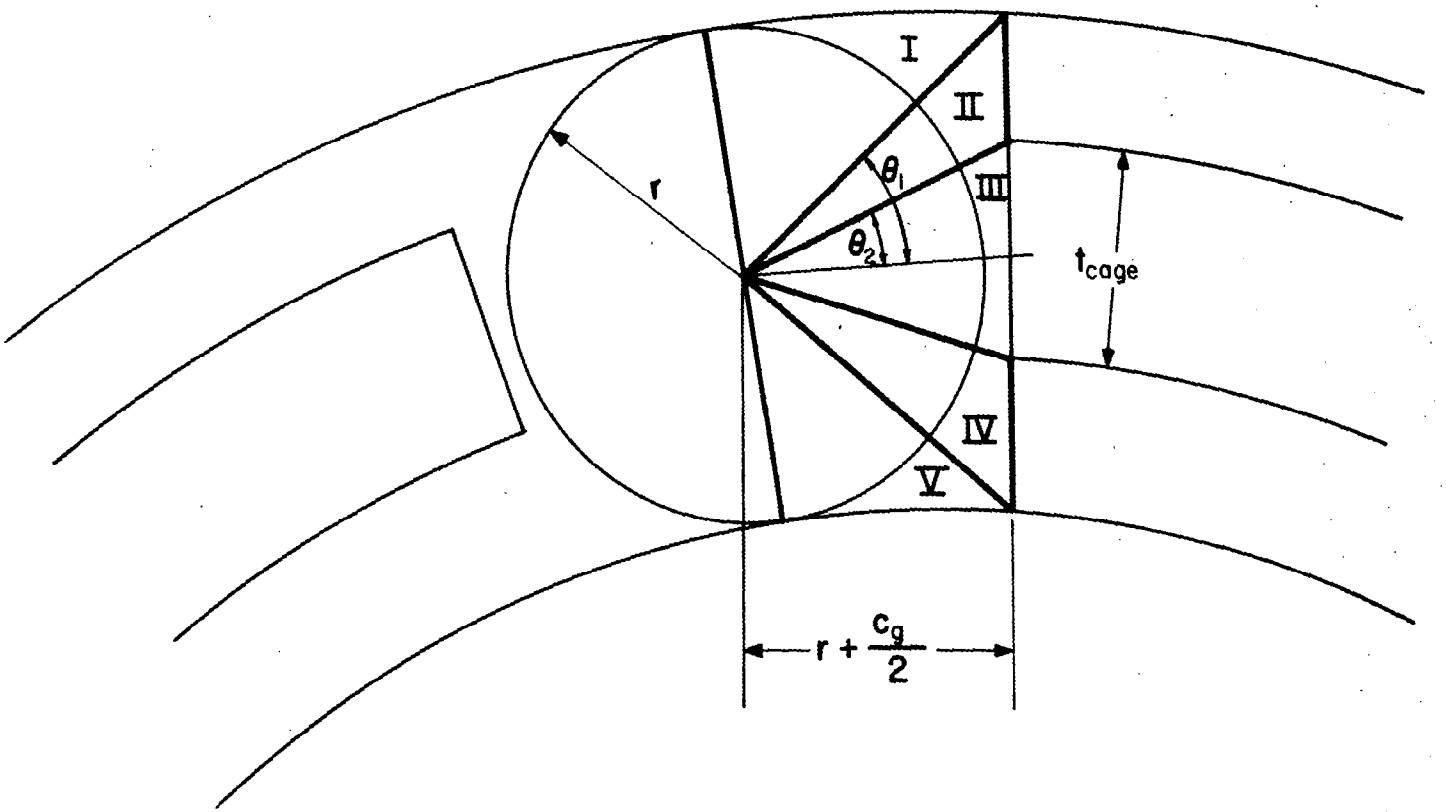

Fig. 8. Model for Computation of the Average Clearance between the Roller and the Cage

and the effective density of the oil/air mixture about the roller for this correlation is

$$\rho_{eff} = \rho \text{ (DECFUL)} \tag{53}$$

If the Reynolds number is less than 2500 or the Taylor number is less than 41, the appropriate friction factor is taken to be the laminar friction factor f_L (equation (30)).

The average shear stress acting on the surface of the roller is

$$\tau_w = \frac{1}{2} f \rho_{eff} \left(\frac{r \dot{\zeta}}{2}\right)^2 \tag{54}$$

where $\dot{\zeta}$ is the angular velocity of the roller about its own axis.

The average drag torque on the roller is calculated by integrating a differential drag torque over the area of the roller, excluding the area between the roller and the cage.

$$T_{DRAG} = \tau_w r^2 \ell (2\pi - 4\theta_2) \tag{55}$$

The expressions given in this section are computed in subroutine R1245 [5].

Drag Torque on the roller ends

Drag torques resist the motion of the roller as it moves through the oil/air mixture as was seen in the previous section. In addition to drag torques on the cylindrical surface, there are drag torques on the roller ends. Following Rumbarger et. al. [3], the effective density of the oil/air mixture is given by equation (53).

The drag torque is computed by using equation (34), supported by equations (32), (33) and (35). The angular velocity to be used is $\dot{\zeta}_i$, the angular velocity of the roller about its own axis.

These relationships are programmed in subroutine ROLEND [5].

Forces between roller end and guiding flange

Roller bearings with the roller guided on the inner race subject the roller to both driving forces and drag forces due to the close clearances and resulting lubrication forces between the roller ends and the guiding flange. The flow field in this location is very complex but a simplified model is used to approximate these forces [3].

The forces in this program are based on the shearing of the lubricant between the roller end and the guiding flange. The roller is assumed to move with equal axial clearance on both sides.

Referring to Figure 9, the area of the roller which projects on the guiding flange is divided into 5 horizontal strips and 8 vertical strips, symmetrical about the vertical line through the center.

The effective density of the oil/air mixture is again given by equation (53).

The forces and torques acting on the strips are calculated from the shear stress acting on the strip in the direction of the strip

$$\tau = \rho_{eff} \nu \frac{\partial u}{\partial y} \qquad (56)$$

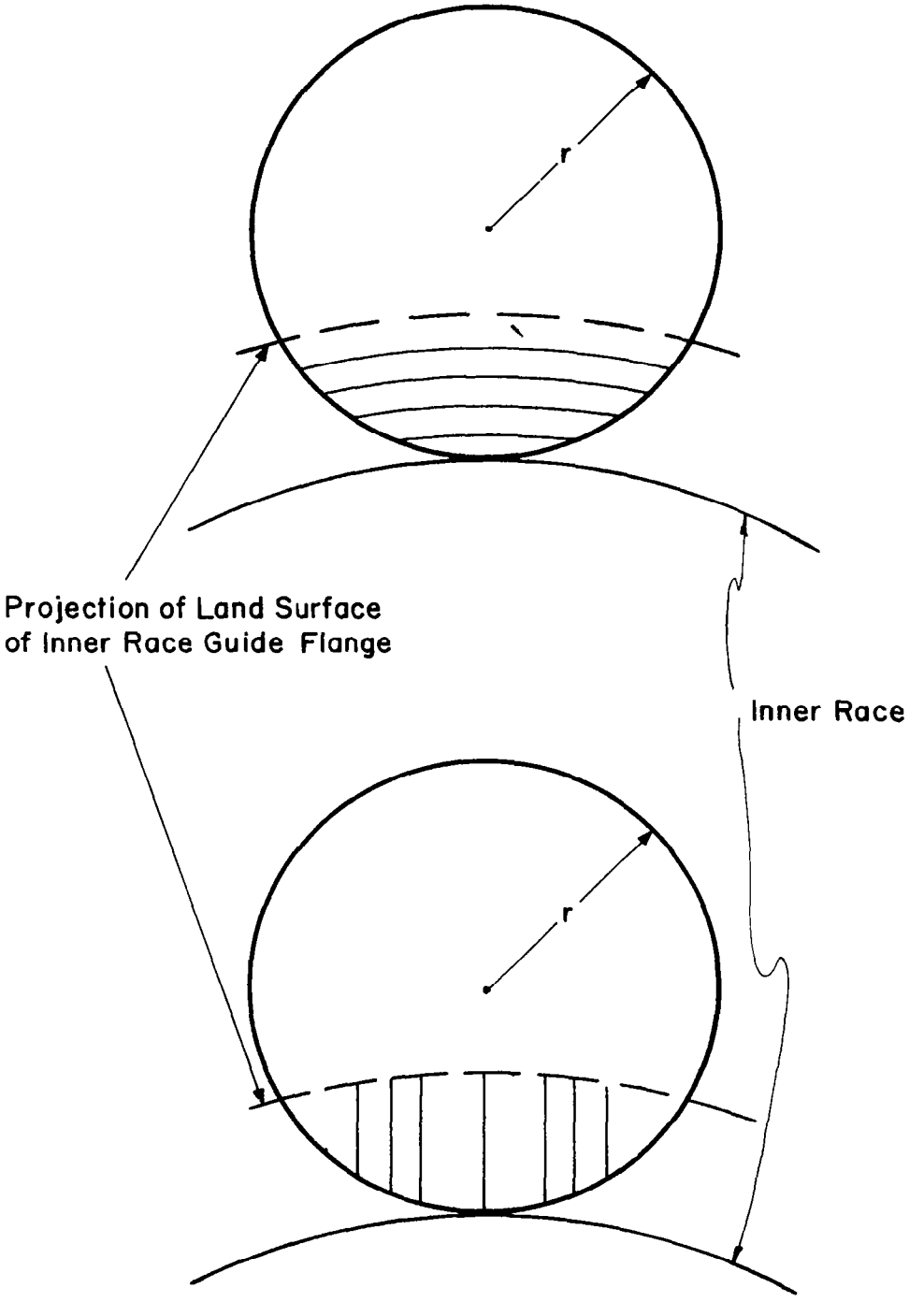

Figure 9. Model for Calculating the Forces Between the Roller End and the Guiding Flange

where $\frac{\partial u}{\partial y}$ is the velocity gradient of the velocity in the direction of the strip.

The driving and retarding forces and torques are calculated in subroutine LANDLIP [5].

THE TWO DIMENSIONAL GOVERNING DIFFERENTIAL EQUATIONS OF MOTION

Consider a roller bearing with (NZ) rollers, guided by a flange attached to the inner race and separated by a cage. The outer race is assumed to be fixed and the inner race is rotating at some angular speed ω_{shaft}.

For the purposes of writing the two dimensional governing differential equations of motion, the following assumptions are made:

(1) The motion of the roller is only in the transverse plane and is only rotational, both about the axis of the roller and about the axis of the bearing. The roller is assumed to be fixed in position between the inner and outer race, and for the case of high speed bearings, the roller is always pressed against the outer race due to the action of the centrifugal forces.

(2) The motion of the cage is only in the transverse plane and is rotational about its own axis and translational in the plane.

From these two sets of assumptions, the number of degrees of freedom for the roller bearing system is:

$$\text{degrees of freedom} = 3 + 2(NZ) \tag{57}$$

For the purposes of this program, the quantities of interest as cage state variables are the angular velocity, angular displacement, the translational velocities and the translational displacements. The quantities of interest as roller state variables are the angular velocities of the rollers about the roller centers and the angular velocities and angular displacements of

the center of the roller with respect to the bearing center. This gives 3(NZ) + 6 state variables which are required to describe the two dimensional motion of the roller bearing. This in turn implies that the solution of 3(NZ) + 6 first order differential equations are required to provide the state variables which describe the motion of the bearing.

The equations of motion are based on the dynamics of rigid bodies. The forces acting on the rigid bodies, the rollers and the cage, may be due to contact or deflection of the surfaces but the deformations are so small, less than 0.1 percent, that the inertial properties are considered to be constant.

The differential equation of motion of the i^{th} roller about its own axis is

$$I \ddot{\zeta}_i = \sum \text{Torques} \tag{58}$$

Referring to Fig. 3, equation (58) becomes

$$\frac{1}{2} m r^2 \ddot{\zeta}_i = r \left[F_{IN}^{(i)} + F_{OUT}^{(i)} - F_{TBR}^{(i)} - F_{TFR}^{(i)} \right] + T_{rland}^{(i)} - T_{rend}^{(i)} - T_{rcyl}^{(i)} \tag{59}$$

$$i = 1, \ldots, NZ$$

where F_{IN} and F_{OUT} are traction forces calculated by equations (24)

F_{TBR} and F_{TFR} are drag forces on the roller exerted by the cage and are calculated by equations (38) or a coulomb friction as determined by the section on roller-cage interaction forces.

T_{rland} is a driving torque exerted by the guide flange on the roller. It is computed in subroutine LANDLIP [5].

T_{rend} is a drag torque acting on the ends of the roller. It is calculated in subroutine ROLEND [5].

T_{rcyl} is a drag torque acting on the surface of the roller. It is calculated in subroutine R1245 [5].

$\ddot{\zeta}_i$ is the angular acceleration of the i^{th} roller about its own axis

m is the mass of the roller

r is the roller radius

The differential equation of motion of the i^{th} roller about the center of the bearing is, considering the roller as a rigid body with the center of mass at the center of the roller:

$$m\,(r + R)^2\,\ddot{\phi}_i = \sum \text{Torques} \qquad (60)$$

where R is the radius of the inner race

Referring to Fig. 3, equation (60) becomes

$$m\,(r + R)^2\,\ddot{\phi}_i = (R + r)\left[F_{IN}^{(i)} - F_{OUT}^{(i)} + F_{B}^{(i)} - F_{F}^{(i)} + F_{HLAND}^{(i)}\right] \quad (61)$$

$$1 = 1, \ldots, NZ$$

The differential equations of motion of the cage describe the planar motion of the cage. As the motion of the cage is limited to three degrees of freedom, the governing equations, relative to a fixed coordinate system, are:

$$m_{cage}\,\ddot{x} = \sum F_x \quad (62)$$

$$m_{cage}\,\ddot{y} = \sum F_y \quad (63)$$

$$I_{cage}\,\ddot{\vartheta} = \sum \text{Torques} \quad (64)$$

where m_{cage} and I_{cage} are the mass and polar moment inertia of the cage respectively.

The quantities $\sum F_x$ and $\sum F_y$ are the sums of forces acting on the cage in the x and y directions respectively. The forces included in these quantities are the hydrodynamic forces between the cage and the inner race land and the forces from the roller-cage interaction. The gravity vector is in the positive y direction.

The forces between the cage and the inner race land are given in equation (49). The roller-cage interaction forces acting on the cage are calculated from equations (36) through (48). Referring to Figs. (3) and (10):

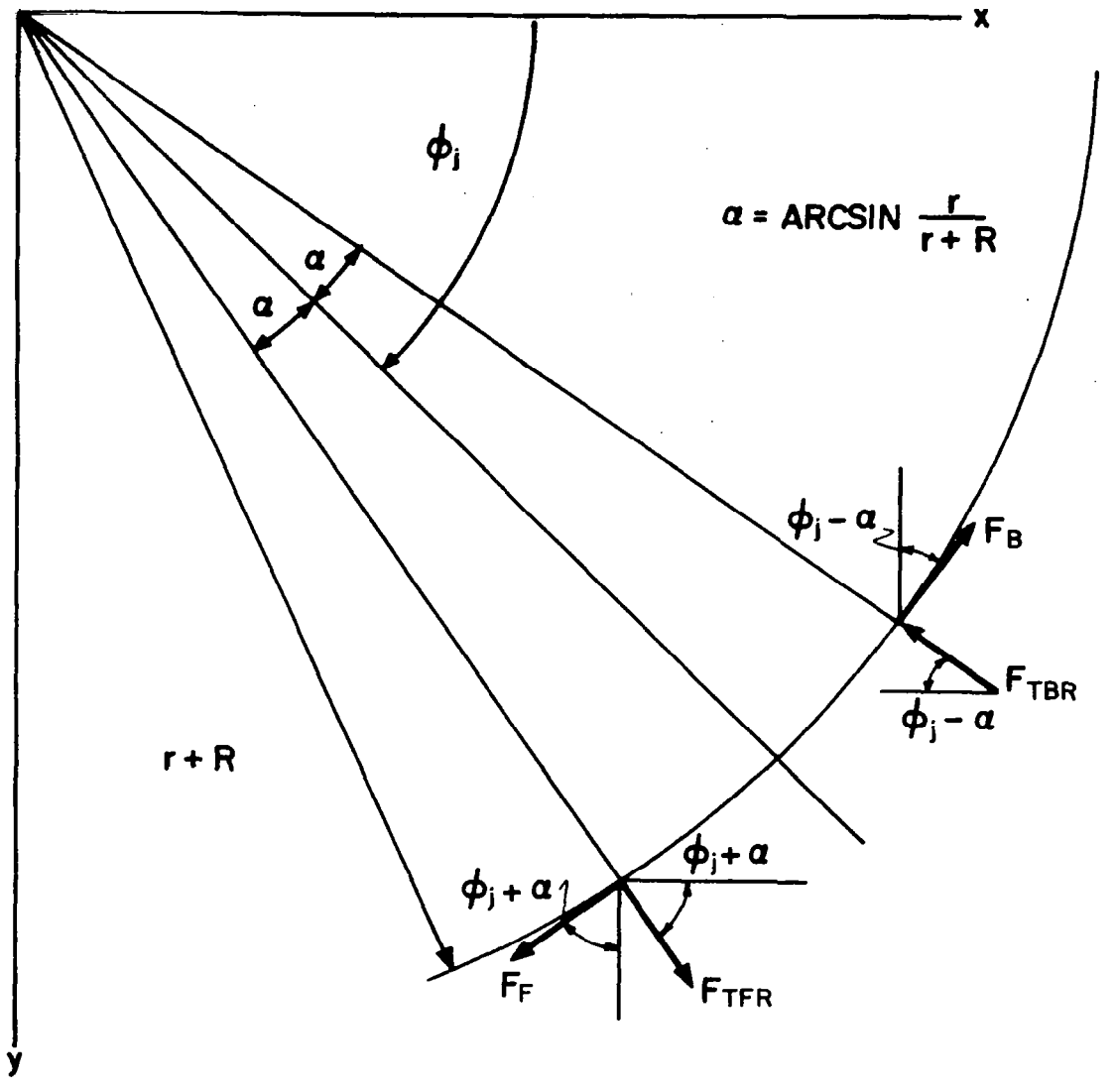

Figure 10. The Normal and Frictional Roller-Cage Forces Acting on the Cage at the j^{th} Pocket

$$\sum F_x = + F_x^{cage} + \sum_{j=1}^{NZ} F_B^{(j)} \sin(\phi_j - \alpha)$$
$$- \sum_{j=1}^{NZ} F_{TBR}^{(j)} \cos(\phi_j - \alpha)$$
$$+ \sum_{j=1}^{NZ} F_{TFR}^{(j)} \cos(\phi_j + \alpha)$$
$$- \sum_{j=1}^{NZ} F_F^{(j)} \sin(\phi_j + \alpha) \qquad (65)$$

$$\sum F_y = + F_y^{cage} + m_{cage}\, g$$
$$- \sum_{j=1}^{NZ} F_B^{(j)} \cos(\phi_j - \alpha)$$
$$- \sum_{j=1}^{NZ} F_{TBR}^{(j)} \sin(\phi_j - \alpha)$$
$$+ \sum_{j=1}^{NZ} F_{TFR}^{(j)} \sin(\phi_j + \alpha)$$
$$+ \sum_{j=1}^{NZ} F_F^{(j)} \cos(\phi_j + \alpha) \qquad (66)$$

The torques which act on the cage are classified into three categories; (1) the torques due to cage-roller interactions, (2) the driving torque due to inner race land-cage interaction, and (3) the drag torques about the sides and outer surface of the cage due to the shearing of the oil-air mixture. The right hand side of equation (64) is written as

$$\sum \text{Torques} = \iint_{\substack{\text{cage-land} \\ \text{area}}} \tau \, r_{IN} \, dA + (R + r) \sum_{j=1}^{NZ} (F_F^{(j)} - F_B^{(j)}) - T_{CDS} - T_{CDO} \tag{67}$$

where T_{CDO} and T_{CDS} are given by equations (25) and (34) respectively.

The shear stress used in the integral in equation (67) is represented as

$$\tau = \frac{\mu \, r_{IN} \, (\omega_{shaft} - \omega_c)}{h} \tag{68}$$

where r_{IN} is the inner radius of the cage which rides on the land

h is the film thickness

μ is the absolute viscosity of the oil

ω_{shaft} is the angular speed of the shaft

ω_c is the angular speed of the cage

Letting

$$h = C \, (1 + \epsilon \cos \theta) \tag{69}$$

the integral in equation (67) becomes:

$$\iint_{\substack{\text{cage land} \\ \text{area}}} \tau \, r_{IN} \, dA = \frac{2 \, \mu \, L \, r_{IN}^3}{C} \, (\omega_{shaft} - \omega_c) \, \frac{2\pi}{\sqrt{1 - \epsilon^2}} \tag{70}$$

where C is the radial clearance between the cage and the land

L is the half width of the total cage-land surface

ϵ is the ratio of the minimum film thickness to the radial clearance

Some of the differential equations described above are reformulated for a more efficient numerical solution. The motion of the center of mass of a roller is necessarily limited by the constraints of the cage pocket. A critical quantity used in the determination of the cage-roller interaction forces is the relative distance between a roller surface and its cage pocket surfaces. This quantity is obtained by subtracting the angular displacement of the mass center of the roller from the angular displacement of the cage, which numbers can become very large and which can lead to errors in accuracy.

Rather than solve equations (61) and (64) and subtract the ϕ_i's from ϑ, equations (61) are replaced by the difference between the angular accelerations of the rollers and the angular acceleration of the cage. When integrated twice this yields an angular displacement difference. The calculation will be stable, the displacement will be bounded and the numerical problem of differencing large numbers will be avoided. The new set of differential equations obtained from equations (61), (64), (67) and (70) are

$$\ddot{\phi}_i - \ddot{\vartheta} = \frac{1}{m\,(r+R)}\left[F_{IN}^{(i)} - F_{OUT}^{(i)} + F_B^{(i)} - F_F^{(i)} + F_{HLAND}^{(i)}\right]$$

$$- \frac{4\pi\ \mu\ L\ \ r_{IN}^{3}\ (\omega_{shaft}\ \omega_c)}{I_{cage}\ C\ \sqrt{1-\epsilon^2}}$$

$$- \frac{(r+R)}{I_{cage}} \sum_{j=1}^{NZ} (F_F^{(j)} - F_B^{(j)})$$

$$+ \frac{T_{CDS}}{I_{cage}} + \frac{T_{CDO}}{I_{cage}} \qquad (71)$$

$$i = 1, \ldots, NZ$$

The governing differential equations for the planar motion of the roller bearing system are now given by equations (59), (62), (63), (64) and (71). These are 2(NZ) + 3 equations which correspond to the number of degrees of freedom given in equation (57).

Before attempting a numerical solution of this system of equations, they will be made non-dimensional. The forces will be scaled by a quantity F* which is taken to be the maximum force on any of the rollers [2]. This maximum force is related to the mass of the roller, a characteristic dimension, in this case, R + r, and a characteristic value of time by

$$m\,(R+r)\,\omega_e^{\,2} = F^* \qquad (72)$$

where ω_e is a characteristic angular velocity

The dimensionless time T is related to real time t by

$$T = \omega_e \, t \tag{73}$$

Equation (71) is related to the relative displacement of the center of the roller in the cage pocket by multiplying it by (R + r) and scaling it with the total clearance between the roller and the cage pocket (C_g). The relative dimensionless displacement is defined as

$$\Delta_i = \frac{(R + r)\ (\phi_i - \vartheta)}{C_g} \tag{74}$$

In addition to scaling forces by F*, torques are scaled by F* r and the dimensionless torques and forces are denoted by a supra bar (-).

Equation (59) becomes

$$\frac{d^2 \zeta_i}{dT^2} = \frac{2\ (r + R)}{r} \left[\bar{F}_{IN}^{(i)} + \bar{F}_{OUT}^{(i)} - \bar{F}_{TBR}^{(i)} - \bar{F}_{TFR}^{(i)} + \bar{T}_{rland}^{(i)} - \bar{T}_{rend}^{(i)} - \bar{T}_{rcyl}^{(i)} \right]$$

$$i = 1, \ldots, NZ \tag{75}$$

Equation (71) becomes

$$\frac{d^2 \Delta_i}{dT^2} = \frac{(r + R)}{C_g} \left\{ \bar{F}_{IN}^{(i)} - \bar{F}_{OUT}^{(i)} + \bar{F}_B^{(i)} - \bar{F}_F^{(i)} + \bar{F}_{HLAND}^{(i)} - \frac{4 \pi \mu L r_{IN}^3}{I_{cage}\ C\ \omega_e \sqrt{1 - \epsilon^2}} \left(\frac{\omega_{shaft}}{\omega_e} - \frac{d\vartheta}{dT} \right) - \frac{m\ (r + R)^2}{I_{cage}} \sum_{j=1}^{NZ} (\bar{F}_F^{(j)} - \bar{F}_B^{(j)}) \right.$$

$$+ \frac{(T_{CDS} + T_{CDO})}{I_{cage}\ \omega_e^2} \Bigg\} \tag{76}$$

$$i = 1, \ldots, NZ$$

Define the dimensionless displacements of the cage as:

$$\bar{x} = \frac{x}{C}$$

$$\bar{y} = \frac{y}{C} \tag{77}$$

Equations (62) and (63) are then given as:

$$\frac{d^2 \bar{x}}{dT^2} = \frac{1}{m_{cage}\ \omega_e^2\ C} \Bigg\{ F_x^{cage} + \sum_{j=1}^{NZ} \Big[F_B^{(j)} \sin(\phi_j - \alpha) - F_{TBR}^{(j)} \cos(\phi_j - \alpha) + F_{TFR}^{(j)} \cos(\phi_j + \alpha) - F_F^{(j)} \sin(\phi_j + \alpha) \Big] \Bigg\} \tag{78}$$

$$\frac{d^2 \bar{y}}{dT^2} = \frac{1}{m_{cage}\ \omega_e^2\ C} \Bigg\{ F_y^{cage} + m_{cage}\ g - \sum_{j=1}^{NZ} \Big[F_B^{(j)} \cos(\phi_j - \alpha) + F_{TBR}^{(j)} \sin(\phi_j - \alpha) - F_{TFR}^{(j)} \sin(\phi_j + \alpha) - F_F^{(j)} \cos(\phi_j + \alpha) \Big] \Bigg\} \tag{79}$$

The differential equation relating the angular acceleration of the cage to the torques acting on the cage (equation (64)) is

$$\frac{d^2\vartheta}{dT^2} = \frac{4\pi\,\mu\,L\,r_{IN}^3}{I_{cage}\,C\,\omega_e\sqrt{1-e^2}}\left(\frac{\omega_{shaft}}{\omega_e} - \frac{d\vartheta}{dT}\right)$$

$$+ \frac{m\,(r+R)^2}{I_{cage}} \sum_{j=1}^{NZ} (\bar{F}_F^{(j)} - \bar{F}_B^{(j)})$$

$$- \frac{(T_{CDS} + T_{CDO})}{I_{cage}\,\omega_e^2} \qquad (80)$$

The system of differential equations (equations (75), (76), (78) (79) and (80))are then solved numerically to obtain the state variables of interest. Equations (75) are only integrated once to find the angular velocity of the roller. The angular displacement of the roller about its own center is not needed for this problem. Equations (76) are integrated twice to find the relative velocity and relative displacement of the roller in the pocket. Equations (78), (79) and (80) are also integrated twice to find the velocities and displacements of the cage.

THE THREE DIMENSIONAL GOVERNING DIFFERENTIAL EQUATIONS OF MOTION

The equations of motion to be presented in this chapter build on the governing equations developed in THE TWO DIMENSIONAL GOVERNING DIFFERENTIAL EQUATIONS OF MOTION. Four more degrees of freedom are added to each roller, an axial translation, a radial translation, a skewing of the roller relative to the inner race and a tilt of the roller relative to the inner race.

The cage motion is assumed to remain planar. The cage in a typical very high speed bearing has a large angular momentum vector which would require torques of high magnitude to force the cage into a significant precession. Kingsbury [18] observed this phenomenon of planar cage motion in tests of bearings for gyroscopes.

The planar model of the cage is also used because of the lack of good models to relate the potentially skewed surfaces between roller and cage to torques about the transverse axes of the cage. The roller is so constrained by the side flanges that, for the purpose of calculating the squeeze film forces, it remains parallel to the cage pocket surface.

In the previous section, the roller motion in the radial direction was constrained to satisfy the static equations of equilibrium of the roller bearing system. In this section, that constraint is relaxed to allow accelerations of the roller in the radial direction because of the cross couplings of the tilt angle of the roller, the radial deflection of the roller and the normal force and tilt torque applied to the roller. These quantities are needed to solve the coupled Euler equations of motion for each

roller. The static equations of equilibrium are used to establish the initial conditions for the roller radial displacements of the centers of mass of the rollers and the roll angles of the rollers.

The complete motion of each roller is obtained by considering the motion of the center of mass of the roller in the inertial coordinate frame (ρ, ϕ, z) and the rotational motion of the roller about its center of mass in the roller frame (ξ, η, ζ) under the assumption that the tilt angle ξ and the skew angle η are very small. These frames are selected such that the ρ vector and the η axis are parallel and the ζ axis is parallel to the inertial axis z.

Denoting the mass of the roller by m, the polar moment of inertia of the roller (about the ζ axis) by I and the transverse moment of inertia of the roller by I_T, the equations of motion of each roller are [19]:

$$
\begin{aligned}
m\,(\ddot{\rho}_i - \rho_i \dot{\phi}_i^2) &= F_{\rho}^{(i)} \\
m\,(\rho_i \ddot{\phi}_i + 2\,\dot{\rho}_i \dot{\phi}_i) &= F_{\phi}^{(i)}
\end{aligned}
\qquad (81)
$$

$$i = 1, \ldots, NZ$$

$$
\begin{aligned}
I_T \ddot{\xi}_i - I_T \dot{\eta}_i \dot{\phi}_i &= G_{\xi}^{(i)} \\
I_T \ddot{\eta}_i + I_T \dot{\xi}_i \dot{\phi}_i &= G_{\eta}^{(i)} \\
I \ddot{\zeta}_i &= G_{\zeta}^{(i)}
\end{aligned}
\qquad (82)
$$

$$i = 1, \ldots, NZ$$

where $\dot{\phi}_i$ is the orbital velocity of the roller

G_ξ, G_η and G_ζ as the torques applied about the (ξ, η, ζ) axis

The third of equations (82) are identical to equations (58). The torques $G_\xi^{(i)}$ are given in the right side of equation (59).

The axial motion of the roller relative to the inner race is determined using a kinematic relationship. The axial velocity of the center of mass of the roller relative to the race is equal to the product of the relative velocity of the center of mass of the roller and the race in the η direction ($U_{rel}^{(i)}$) and the angle of skew of the roller (η_i), thus

$$\frac{dz_i}{dt} = U_{rel}^{(i)} \eta_i \qquad (83)$$

$$i = 1, \ldots, NZ$$

The radius vector ρ_i in equations (81) is given as

$$\rho_i = r + R + \delta_r^{(i)} \qquad (84)$$

where $\delta_r^{(i)}$ is the deflection of the roller mass center and r and R are the roller radius and inner race radius respectively.

The forces $F_\rho^{(i)}$ are determined by substituting the $\delta_r^{(i)}$ for $\delta\phi_j$ and the η_i for β_j in equations (4), (5), and (10) with $F_C = 0$. The residual F_j is interpreted as the net applied force on the roller in the radial direction. The torques, $G_\xi^{(i)}$, are determined by evaluating equation (11) where the residual, F_{j+NZ}, is the negative of the net tilt torque on the roller.

The dimensionless form of the forces, $F^{(i)}$, are given in the brackets on the right hand side of equations (61). If ρ_i were a constant, the second of equations (81) would be identical to equations (61).

The torques $G_{\eta}^{(i)}$ in equations (82) have two components, a torque due to unevenly distributed traction forces along the length of the roller at the roller-race interfaces and a torque due to elastic deformation between the edges of the roller and the guiding flanges of the inner race when the roller impacts those guide flanges. The torque due to unevenly distributed traction forces is continuous in time. The misalignment of the bearing inner race to the outer race contributes to the uneven load distribution on the roller which in turn affects the magnitude of the traction coefficient. The net moment of the product of the normal loads on the "slices" of the roller (from Chapter 2) and the traction coefficients for the same slices is the torque which tends to skew the roller.

The torque due to the impact of the roller edge(s) with the guide flange(s) gives rise to a restoring torque which can have a large magnitude. The basis for calculating the contact force is given by Brewe and Hamrock [20] where an approximate force relationship is given as a function of the geometry of the contacting surfaces and the material constants.

$$F_I = \left[\left(\frac{\delta}{f}\right)^3 \left(2R_{eff}\psi\right)\right]^{1/2} \left(\frac{\pi k E'}{3}\right) \tag{85}$$

$$\text{where } f = 1.5277 + 0.6023 \log_e (R_y/R_x) \tag{86}$$

$$\frac{R_y}{R_x} \geq 1 \tag{87}$$

$$\psi = 1.0003 + \frac{0.5968}{R_y/R_x} \tag{88}$$

$$\frac{1}{R_{eff}} = \frac{1}{R_x} + \frac{1}{R_y} \tag{89}$$

$$\frac{1}{R_x} = \frac{1}{r_{Ax}} + \frac{1}{r_{Bx}} \tag{90}$$

$$\frac{1}{R_y} = \frac{1}{r_{Ay}} + \frac{1}{r_{By}} \tag{91}$$

$$k = 1.0339 \left(\frac{R_y}{R_x}\right)^{0.6360} \tag{92}$$

$$E' = 2\left[\frac{1 - \nu_A^2}{E_A} + \frac{1 - \nu_B^2}{E_B}\right]^{-1} \tag{93}$$

where F_I is the contact force due to impact

δ is the contact deflection

f is an approximation of an elliptic integral of the second kind

R_{eff} is the effective radius

r_{Ax} etc. are radii of curvature

k is the ellipticity parameter

ν is Poisson's ratio

ψ is an approximation of an elliptic integral of the first kind

E' is the effective modulus of elasticity

The subscripts A and B refer to the two bodies in contact, respectively.

The equivalent radius in one principal plane at the contact point is approximated as:

$$\frac{1}{R_x} = \frac{1}{r_m} \tag{94}$$

The equivalent radius in the other principal plane at the contact point is approximated as:

$$\frac{1}{R_y} = \frac{1}{r_{fm}} \tag{95}$$

Therefore from equations (89), (94) and (95)

$$\frac{1}{R_{eff}} = \frac{1}{r_{fm}} + \frac{1}{r_m} \tag{96}$$

where r_m is the minor radius at the corner of the roller

r_{fm} is the minor radius of the inner race guide flange at the corner.

When the roller is skewed, the contact between the roller and the guide flange is at a point located at the intersection of the roller circumference and the circumference of outer surface of the guide flange.

The restoring torque after impacting the guide flange is

$$T_f = r_f F_I \tag{97}$$

as shown in figures (4) and (11). Figure (11) also illustrates that

$$r_f = r \sin \Theta_F$$
$$\Theta_F = \arccos \left[\frac{(R + r)^2 + r^2 - R_f^2}{2r (R + r)} \right] \tag{98}$$

where R_f is the radius of the outer surface of the inner race guide flange

In summary, the torques $G_\eta^{(i)}$ may be expressed as:

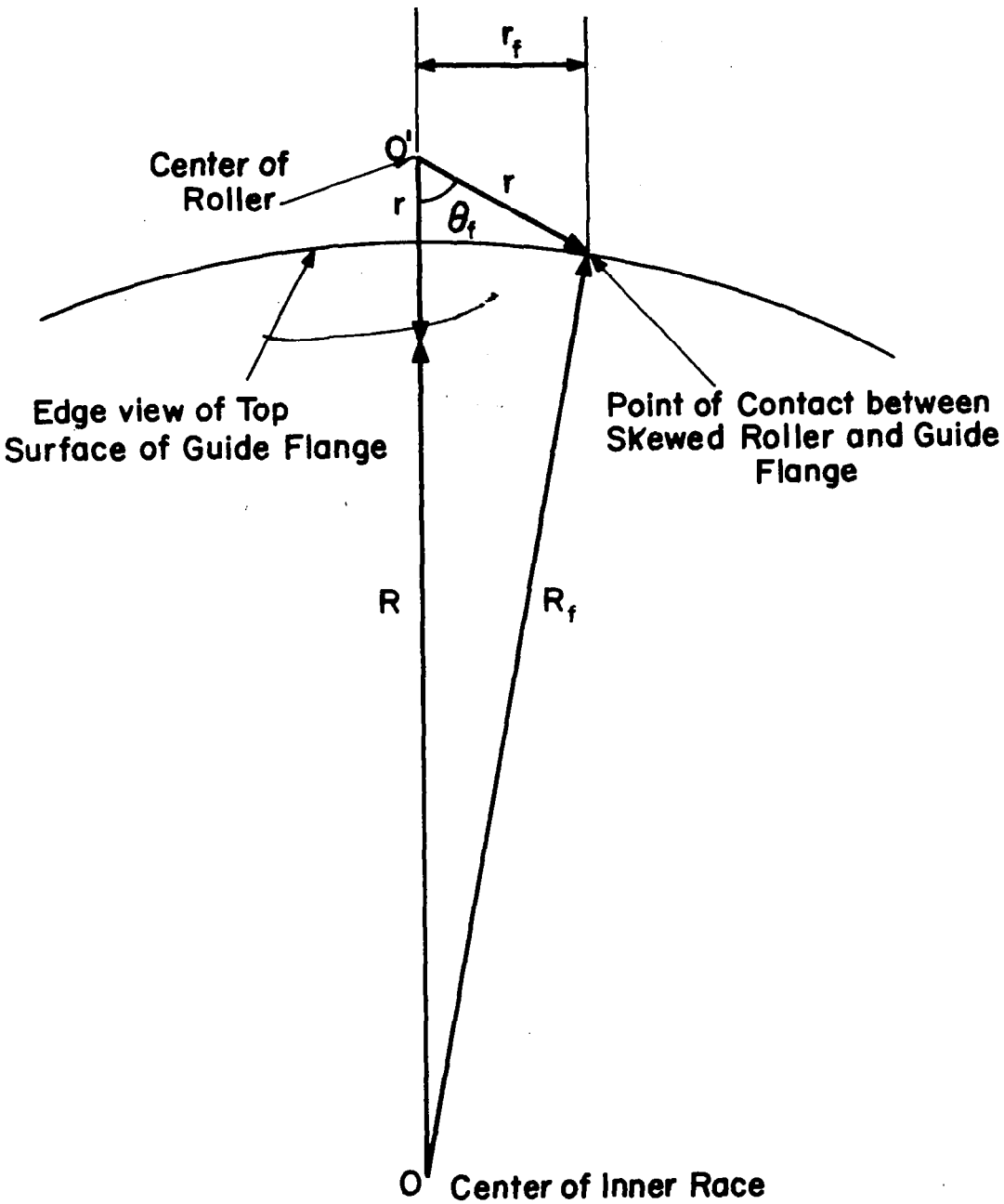

Figure 11. The Geometry of the Roller Bearing System Used to Establish the Point of Contact Between a Skewed Roller and the Guide Flange

$$G_{\eta}^{(i)} = \sum_{j=1}^{NP} z^{(j)} \left(F_{IN}^{(ij)} - F_{OUT}^{(ij)} \right) + \sum_{j=1}^{4} r_f F_I^{(j)} \qquad (99)$$

where $z^{(j)}$ is the distance from the center of mass of the roller to the center of the "slice" as described in THE CONSTITUENT MODELS.

$F_{IN}^{(ij)}$ and $F_{OUT}^{(ij)}$ are the tractive forces calculated over the contact area of the j 'th slice using equations (24)

$F_I^{(j)}$ is the contact force between a roller corner and the side walls of the guide flange.

In equation (99) the four potential contact points of the roller are considered, Fig. 4. In the program, the locations of these points are monitored and if contact occurs, the corresponding $F_I^{(j)}$ is calculated. If there is no contact, the corresponding $F_I^{(j)}$ is set to zero.

From the discussion presented thus far in this chapter, ten first order differential equations are required to describe the motion of each roller. For the bearing with NZ rollers and a cage in planar motion only, the total number of first order differential equations is 6 + 10 (NZ).

The remainder of this section deals with the simplifications made to this system of equations. The essential character of the motion is retained while ignoring some smaller effects.

Consider now an harmonic solution of the first of equations (81), after the substitution of equation (84) to be

$$\delta_r^{(i)} = D_1 \cos \dot{\phi}_i t \tag{100}$$

Then

$$m \left(- D_1 \dot{\phi}_i^2 \cos \dot{\phi}_i t - (R + r) \dot{\phi}_i^2 - D_1 \dot{\phi}_i^2 \cos \dot{\phi}_i t \right) = F_\rho^{(i)} \tag{101}$$

The quantity on the left hand side is dominated by the term (R + r), since

$$R + r \gg D_1 \tag{102}$$

The value of D_1 would typically be of the order of 10^{-3} or 10^{-2} and R + r is of the order 1. This implies that the forces $F_\rho^{(i)}$ should be equal to the centrifugal forces, the condition enforced in the static load distribution problem considered in THE CONSTITUENT MODELS. Thus the first of equations (81) may be eliminated.

At each point in time every roller is placed in static equilibrium which implies that the velocity and acceleration of the center of mass of the roller are zero in the radial direction. Thus, the second of equations (81) become, using equation (102)

$$m (r + R) \ddot{\phi}_i = F_\phi^{(i)} \tag{103}$$

$$i = 1, \ldots, NZ$$

Equations (103) are identical to equations (61).

The first of equations (82) are eliminated because of the enforcement of the static equations of equilibrium. The torques $G_{\xi}^{(i)}$ are zero as a result of this constraint and the values of the roll velocity and acceleration of the rollers are taken to be zero. The second term of the first of equations (82), $-I_T \dot{\eta}_i \dot{\phi}_i$, is estimated to have a magnitude of the order of 1.13×10^{-2} N-m (10^{-2} in - lb_f) which would entail only a minute change in the static normal load distribution of the rollers.

The second term on the left hand side of the second of equations (82) is set to zero because of assumption of zero tilt velocity and acceleration of the rollers. This set of differential equations for the skew displacements becomes:

$$I_T \ddot{\eta}_i = G_{\eta}^{(i)} \qquad (104)$$

$$i = 1, \ldots, NZ$$

The simplified system of governing differential equations for the three dimensional motion of the rollers is given by the third of equations (82), equations (83), (103) and (104). The equations of motion of the cage remain unchanged from the planar motion case.

The dimensionless form of equations (83) is then written as using equations (73) and (74)

$$\frac{d\,\bar{z}_i}{dT} = -\left[\frac{\dot{\Delta}_i\, C_g}{C_z} + \frac{\dot{\phi}\,(R + r)}{C_z} - \frac{R\,\omega_{shaft}}{C_z}\right] \eta_i \qquad (105)$$

where $\bar{z}_i = \dfrac{z_i}{C_z}$

C_z is the total axial clearance between the roller ends and the inner race guide flanges

ω_{shaft} is the shaft angular velocity

The dimensionless form of equations (104) for the skew displacements are of the form

$$\frac{d^2 \eta_i}{dT^2} = \frac{F^*}{I_T \omega_e^2} \sum_{j=1}^{NP} z^{(j)} (\bar{F}_{IN}^{(ij)} - \bar{F}_{OUT}^{(ij)})$$

$$+ \frac{F^*}{I_T \omega_e^2} \sum_{j=1}^{4} r_f \bar{F}_I^{(j)} \qquad (106)$$

The reduced system of dimensionless differential equations to be solved is equations (75), (76), (78), (79), (80), (105) and (106).

DISCUSSION OF RESULTS

The equations of motion developed in this report differ in certain respects from those presented by Gupta [4]. Gupta presents the three equations of motion of the roller mass center in an inertial reference frame and presents the three Euler equations of motion in a roller fixed frame. He then presents a transformation matrix to convert the moments from an inertial frame to a roller fixed frame. His formulation is generalized and contains the full six degrees of freedom for each roller.

Two formulations of the equations of motion were presented in this report, the two dimensional problem and the three dimensional problem. The motion of the cage is limited to two dimensions for both cases. The two dimensional formulation only permits planar motion of the roller. The radial motion is neglected as the races and centrifugal forces effectively constrain it to be very small.

The three dimensional formulation again neglects the radial displacement and the tilt angle dynamics of the roller. The tilt of the roller is assumed to be a function of the misalignment of the races, the loading, and the geometry and elasticity of the rollers. The axial motion of the roller relative to the race is expressed by a kinematic condition rather than a dynamic condition.

The equations of motion which describe the motion of the roller center in the plane of the bearing are modified in this report. Many of the forces which act on the cage and the rollers are functions of the relative displacements between roller and cage. To keep numerical stability, new differential equations are formulated in terms of these relative displacements. Gupta [4] makes no mention of using this approach.

The approach used by Gupta [4] for calculating roller-race interaction is essentially the same as used in this report. The work of Palmgren [8] was used as the basis for the normal load distribution calculation. The lubricant model used in this report was for Mil-L-7808 type lubricant while Gupta [4] used Mil-L-7808 and 5P4E polyphenyl ether.

The roller end to race flange interactions are treated in similar fashion in this report and in Ref. [4]. The roller to cage and race to cage interactions are also treated in a similar fashion to Ref. [4]. The churning and drag loss models in this report and in [4] are based on the work of Rumbarger [3]. These are approximate models which depend on an effective density. This approach has been used in most rolling bearing applications. The effective oil density is in effect a parameter which must be adjusted to the operating conditions which are being simulated.

CONCLUDING REMARKS

The two and three dimensional differential equations of motion of a high speed cylindrical roller bearing have been derived in this report. Simplifying assumptions were made which were specific to the cylindrical roller bearing. The original differential equations were manipulated to provide a more numerically stable system of differential equations.

Approximate models were utilized to compute churning losses, traction forces, roller to cage and roller to race interaction forces. As more knowledge becomes available in these specific areas, changes to the overall differential equations can be made.

REFERENCES

1. Walters, C.T., "The Dynamics of Ball Bearings," Journal of Lubrication Technology, Trans. ASME, Series F, Vol. 93, no. 1 (1971) pp. 1-10.

2. Gupta, P.K., "Transient Ball Motion and Skid in Ball Bearings," Journal of Lubrication Technology, Trans. ASME, Series F, Vol. 97, no. 2 (1975) pp. 261-269.

3. Rumbarger, J.H., Filetti, E.G. and Gubernick, D., "Gas Turbine Mainshaft Roller Bearing-System Analysis," Journal of Lubrication Technology, Trans. ASME, Series F, Vol. 95, no. 4 (1973) pp. 401-416.

4. Gupta, P.K., "Dynamics of Rolling Element Bearings, Part I, Part II", Journal of Lubrication Technology, Trans. ASME, Vol. 101, no. 3 (1979) pp. 293-311.

5. Conry, T.F. and Goglia, P.R., Transient Dynamic Analysis of High-Speed Lightly Loaded Cylindrical Roller Bearings. II - Computer Program and Results, NASA CR-3335, 1980.

6. Harris, T.A., "The Effect of Misalignment on the Fatigue Life of Cylindrical Roller Bearings Having Crowned Rolling Members," Journal of Lubrication Technology, Trans. ASME, Vol. 91, Series F, no. 2 (1969) pp. 294-300.

7. Liu, J.Y., "The Effect of Misalignment on the Life of High Speed Cylindrical Roller Bearings," Journal of Lubrication Technology, Trans. ASME, Vol. 93, Series F, no. 1 (1971) pp. 60-68.

8. Palmgren, G., "Cylinder Compressed Between Two Plane Bodies," SKF Aktiebolaget Svenska Kullagerfabriken, Goteborg, August 1949.

9. Johnson, K.L. and Tevaarwerk, J.L., "Shear Behaviour of Elastohydrodynamic Oil Films," Proc. Royal Society London, Series A, Vol. 356, pp. 215-236 (1977).

10. McCool, J. I., "Influence of Elastohydrodynamic Lubrication on the Life and Operation of Turbine Engine Ball Bearings," Interim Technical Report, October 1, 1973, SKF Industries Inc.

11. Boness, R.J., "The Effects of Oil Supply on Cage and Roller Motion on Lubricated Roller Bearings," Journal of Lubrication Technology, Trans. ASME, Series F, Vol. 92, no. 1 (1970) pp. 39-53.

12. Poplawski, J.V., "Slip and Cage Forces in a High-Speed Roller Bearing," Journal of Lubrication Technology, Trans. ASME, Series F. Vol. 94, no. 2 (1972) pp. 143-152.

13. Schlichting, H., Boundary Layer Theory, 4th edition, McGraw-Hill Book Company, 1960.

14. Dowson, D., Markho, P.H. and Jones, D.A., "The Lubrication of Lightly Loaded Cylinders in Combined Rolling, Sliding and Normal Motion, Part I: Theory," Journal of Lubrication Technology, Trans. ASME, Series F, Vol. 98, no. 4 (1976) pp. 509-516.

15. Loo, T.T., "Effect of Curvature On The Hertz Theory For Two Circular Cylinders In Contact," Journal of Applied Mechanics, Trans. ASME, Vol. 80, (1958) pp. 122-124.

16. Conry, T.F. and Seireg, A., "A Mathematical Programming Technique for the Evaluation of Load Distribution and Optimal Modifications for Gear Systems," Journal of Engineering for Industry, Trans. ASME, Volume 95, Series B, 1973, pp. 1115-1122.

17. Kirk, R.G. and Gunter, E.J., Transient Journal Bearing Analysis, NASA CR-1549, June 1970.

18. Kingsbury, E.P., "Torque Variations in Instrument Ball Bearings," ASLE Transactions, Vol. 8 (1965) pp. 435-441.

19. McCuskey, S.W., An Introduction to Advanced Dynamics, Addison Wesley Publishing Company, Reading, Mass. (1959).

20. Brewe, D.E. and Hamrock, B.J., "Simplified Solution for Elliptical Contact Deformation Between Two Elastic Solids," Journal of Lubrication Technology, Trans. ASME, Series F, Vol. 99, no. 4 (1977) pp. 485-487.

LIST OF SYMBOLS

SYMBOLS

c	radial clearance (m)
d	distance between edge of cage pocket to center of roller (m)
f	approximation of an elliptic integral of the second kind
f	traction force (N)
f	friction factor
g	acceleration of gravity (m/s^2)
g_{1ij}	total contact deformation at the inner contact of the i^{th} slice of the roller at angular location ϕ_j (m)
g_{2ij}	total contact deformation at the outer contact of the i^{th} slice of the roller at angular location ϕ_j (m)
h	film thickness (m)
h_o	minimum film thickness (m)
k	ellipticity parameter
ℓ	length of a roller (m)
m	mass of a roller (kg)
m_{cage}	mass of the cage (kg)
n	normal load per unit length (N/m)
q	dimensionless velocity parameter
$\bar{q}$	load intensity (N/m)
q_o	maximum Hertzian contact pressure (N/m^2)

r	roller radius (m)
r_c	characteristic radius (m)
r_f	distance as described in equation (98) (m)
r_{fm}	minor radius of the inner race guide flange at the corner (m)
r_{IN}	inner radius of cage (m)
r_m	minor radius at the corner of the roller (m)
r_{OUT}	outer radius of cage (m)
u	mass average velocity of fluid, equation 26 (m/s)
u	entraining velocity (m/s)
u_s	sliding velocity at the roller-race contact (m/s)
u_s^*	normalizing constant for sliding velocity (m/s)
v	rolling velocity at the roller-race contact (m/s)
$\bar{v}$	dimensionless sliding ratio
w	width of a slice of the roller (m)
w	normal velocity (m/s)
w_H	normal indentation of a roller (m)
x	absolute displacement of cage in x-direction (m)
y	absolute displacement of cage in y-direction (m)
Z_i	location of the i^{th} slice of the roller (m)

A	constant equal to 5.46×10^{-8}, equation (1)
A	surface area (m^2)
B	constant, equations (40) and (41)
C	constant, equations (42) and (43)
C	radial clearance (m)
C_g	circumferential clearance in the cage pocket (m)
C_H	average clearance between roller and cage (m)
C_i	initial separation due to crowning of the i^{th} slice of a roller (m)
C_N	friction factor, equation (35)
C_z	axial clearance between roller ends and the inner race guide flanges (m)
D_1	an arbitrary constant
DECFUL	ratio of the oil volume in the bearing to the total volume of the bearing
E	modulus of elasticity (N/m^2)
E'	effective modulus of elasticity (N/m^2)
F*	maximum force on the rollers, used for scaling (N)
F_B	normal forces on the roller exerted by the cage (N)
F_c	centrifugal force on a roller (N)
F_{cage}	dimensionless traction force acting on cage pocket surface
F_F	normal forces on the roller exerted by the cage (N)
F_{HLAND}	force exerted on the roller sides by the inner race land (N)

F_I	contact force due to impact (N)
F_{IN}	traction force between roller and inner race (N)
F_j	residual quantity used in equations (9) and (10)
F_{OUT}	traction force between roller and outer race (N)
F_{roller}	dimensionless traction force acting on roller
F_{TBR}	drag forces on the roller exerted by the cage (N)
F_{TFR}	drag forces on the roller exerted by the cage (N)
F_x	hydrodynamic force on cage in x-direction (N)
F_y	hydrodynamic force on cage in y-direction (N)
G	torque (N-m)
H_o	dimensionless minimum film thickness
I	mass moment of inertia of roller about its axis of rotation (kg - m^2)
I_{cage}	mass moment of inertia of cage (kg - m^2)
I_T	transverse moment of inertia of roller (kg - m^2)
L	half-width of total cage/land surface (m)
N	dimensionless normal load carrying capacity
$N_{in}^{(j)}$	total normal force on the j^{th} roller at the inner race contact (N)
$N_{out}^{(j)}$	total normal force on the j^{th} roller at the outer race contact (N)
NP	number of slices along the axis of roller
N_{RE}	Reynolds number
N_{TA}	Taylor number
NZ	number of rollers in bearing

P'	normal force per unit width (N/m)
P_d	diametral clearance of the bearing (m)
Q	applied load to a roller (N)
R	radius of the inner race (m)
R_{eff}	effective radius
R_{eq}	equivalent radius (m)
R_f	radius of the outer surface of the inner race guide flange (m)
T	dimensionless time
T_{CDO}	drag torque on outer cylindrical surface of cage (N - m)
T_{CDS}	drag torque on the sides of the cage (N - m)
T_f	restoring torque (N - m)
T_{rcyl}	drag torque acting on the surface of the roller (N - m)
T_{rend}	drag torque acting on the ends of the roller (N -m)
T_{rland}	driving torque exerted by the guide flange on the roller (N - m)
U	surface velocity (m/s)

α	one-half of the included angle of the cage pocket (radian)
β_j	tilt angle of the j^{th} roller (radian)
δ	contact deformation (m)
δ_{ϕ_j}	relative approach between the roller axis and the outer ring along the radial line passing through the center of the roller at angular location ϕ_j (m)
ϵ	eccentricity ratio
η	principal axis in roller frame
η	angle of skew (radian)
ϑ	angular displacement of the cage (radian)
μ	dynamic viscosity of oil ($N\text{-}s/m^2$)
μ	traction coefficient
μ^*	normalizing constant for traction coefficient
ν	oil viscosity (m^2/s)
ν	Poisson's ratio
ξ	principal axis in roller frame
ξ	angle of tilt (radian)
ρ	radial direction of roller motion in an inertial frame
ρ_j	displacement of j^{th} roller in the radial direction (m)
ρ	density (kg/m^3)
ρ_{eff}	effective density of oil/air mixture (kg/m^3)
τ	shear stress (N/m^2)
τ_w	wall shear stress (N/m^2)

ϕ_j	angular position of the j^{th} roller relative to the x-axis (radian)
$\dot{\zeta}_i$	angular velocity of the i^{th} roller about its own axis (m/s)
ζ	principal axis in the roller frame
ω	angular velocity
ω_c	angular velocity of the cage (radian/s)
ω_e	characteristic angular velocity, equation (72) (radian/s)
ω_{shaft}	angular velocity of the shaft (radian/s)
Γ	constant, equation (11)
Δ_x	component of radial displacement of bearing inner race in x-direction (m)
Δ_y	component of radial displacement of bearing inner race in y-direction (m)
θ_x	angular misalignment of bearing inner race relative to the outer race about the x-axis (radian)
θ_y	angular misalignment of bearing inner race relative to the outer race about the y-axis (radian)
Φ_o	angular location of an axis with respect to the x-axis about which the total angular misalignment is applied (radian)
ψ	approximation of an elliptic integral of the first kind
Ω	angular velocity (radian/s)

Subscripts

L	laminar
ζ	ζ direction
ξ	ξ direction
η	η direction
ρ	ρ direction
ϕ	ϕ direction
z	z direction

1. Report No. NASA CR-3334	2. Government Accession No.	3. Recipient's Catalog No.
4. Title and Subtitle TRANSIENT DYNAMIC ANALYSIS OF HIGH-SPEED LIGHTLY LOADED CYLINDRICAL ROLLER BEARINGS I - ANALYSIS		5. Report Date January 1981 6. Performing Organization Code
7. Author(s) Thomas F. Conry		8. Performing Organization Report No. None 10. Work Unit No.
9. Performing Organization Name and Address University of Illinois at Urbana-Champaign Urbana, Illinois		11. Contract or Grant No. NSG-3098 13. Type of Report and Period Covered Contractor Report
12. Sponsoring Agency Name and Address National Aeronautics and Space Administration Washington, D.C. 20546		14. Sponsoring Agency Code

15. Supplementary Notes

Lewis Technical Monitor: Harold H. Coe
Final Report

16. Abstract

The governing differential equations of motion for a high speed cylindrical roller bearing are developed under the assumptions that the bearing is isothermal and that the roller tilt and skew are very small. Two sets of differential equations are presented; the first which deals with planar motion of the roller bearing system, and the second which includes the effect of roller skewing. The equations as presented are in a format for programming on a digital computer.

17. Key Words (Suggested by Author(s))		18. Distribution Statement
Bearings	Computer program	Unclassified - Unlimited
Rolling element	Analysis	
Cylindrical roller	Dynamic	Subject Category 37

19. Security Classif. (of this report)	20. Security Classif. (of this page)	21. No. of Pages	22. Price*
Unclassified	Unclassified	80	A05

* For sale by the National Technical Information Service, Springfield, Virginia 22161

NASA-Langley, 1981